AD-A024 711

THEORETICAL ANALYSIS OF ATJS GRAPHITE DISKS FRACTURED BY SPINNING

CALIFORNIA UNIVERSITY

PREPARED FOR

OFFICE OF NAVAL RESEARCH

MARCH 1976

UCLA-ENG-7824
MARCH 1976

THEORETICAL ANALYSIS OF ATJS GRAPHITE DISKS
FRACTURED BY SPINNING

S.B. BATDORF

REPORT DOCUMENTATION PAGE		READ INSTRUCTIONS BEFORE COMPLETING FORM
1. REPORT NUMBER UCLA-ENG-7624	2. GOVT ACCESSION NO.	3. RECIPIENT'S CATALOG NUMBER
4. TITLE (and Subtitle) THEORETICAL ANALYSIS OF ATJS GRAPHITE DISKS FRACTURED BY SPINNING		5. TYPE OF REPORT & PERIOD COVERED Technical 1975-1976
		6. PERFORMING ORG. REPORT NUMBER UCLA-ENG-7624
7. AUTHOR(s) S. B. Batdorf		8. CONTRACT OR GRANT NUMBER(s) N00014-76-C-0445
9. PERFORMING ORGANIZATION NAME AND ADDRESS School of Engineering and Applied Science University of California Los Angeles, California		10. PROGRAM ELEMENT, PROJECT, TASK AREA & WORK UNIT NUMBERS
11. CONTROLLING OFFICE NAME AND ADDRESS Department of Navy		12. REPORT DATE March 1976
		13. NUMBER OF PAGES 47
14. MONITORING AGENCY NAME & ADDRESS(if different from Controlling Office) Office of Naval Research – Branch Office 1030 E. Green St. Pasadena, Ca. 91101		15. SECURITY CLASS. (of this report) Unclassified
		15a. DECLASSIFICATION/DOWNGRADING SCHEDULE

16. DISTRIBUTION STATEMENT (of this Report)

Distribution is unlimited

17. DISTRIBUTION STATEMENT (of the abstract entered in Block 20, if different from Report)

18. SUPPLEMENTARY NOTES

19. KEY WORDS (Continue on reverse side if necessary and identify by block number)

Fracture
Brittle Fracture
Fracture Statistics
Polyaxial Stress –
  Strain Relations

Graphite Fracture
Strength Theories

20. ABSTRACT (Continue on reverse side if necessary and identify by block number)

In a recent experimental investigation of ATJS disks spun to failure, maximum strains at fracture were compared with predictions based on the Weiler-OASIS and Jones-Nelson polyaxial stress-strain relations. In addition the fracture data were analyzed to determine approximate failure vs. strain curves for a number of stress ratios.

The present paper shows that improved strain predictions are obtained using a stress strain relation proposed by the present author. The paper

DD FORM 1473 EDITION OF 1 NOV 65 IS OBSOLETE
S/N 0102 LF 014-6601

also shows how the statistical theory of fra ture under combined stresses can be employed to deduce the uniaxial as well as improved biaxial stress or strain failure relations for the particular graphite used.

THEORETICAL ANALYSIS OF ATJS GRAPHITE DISKS FRACTURED BY SPINNING

S. B. Batdorf

School of Engineering and Applied Science
University of California
Los Angeles, California

ABSTRACT

In a recent experimental investigation of ATJS disks spun to failure, maximum strains at fracture were compared with predictions based on the Weiler-OASiS and Jones-Nelson polyaxial stress-strain relations. In addition the fracture data were analyzed to determine approximate . ilure vs. strain curves for a number of stress ratios.

The present paper shows that improved strain predictions are obtained using a stress strain relation proposed by the present author. The paper also shows how the statistical theory of fracture under combined stresses can be employed to deduce the uniaxial as well as improved biaxial stress or strain failure relations for the particular graphite used.

Table of Contents

List of Figures

INTRODUCTION

Refractory materials are frequently used in reentry vehicle nosetips to combat the severe heating conditions encountered. The thermal stresses thereby induced introduce a risk of fracture. To calculate the surviv. probability, it is necessary to be able to determine the stresses and strains induced by the combined thermal and aerodynamic loads, to find the probability of fracture in each volume element, and from the latter to estimate the survival probability of the entire nosetip. Among the things needed to accomplish this task are sufficiently accurate constitutive laws for the materials employed, and a knowledge of the fracture statistics of the material as affected by specimen size and the (generally biaxial or triaxial) stress state involved.

In a recent experimental study[1] to shed light these matters, ATJS graphite disks and bars were tested to destruction by spinning. The centrifugal forces produced biaxial stresses which varied with the position in the disk. Since only strains (not stresses) could be measured direc ly, such tests furnish a limited but nevertheless useful means of checking the adequacy of various proposed polyaxial stress-strain relations. In addition, the experiments provide data on the statistics of fracture under polyaxial loading conditions.

In Reference 1, strains measured at the center of the disk were checked against theoretical predictions of two different theoretical constitutive laws. In turned out that one theory generally overestimated the strains, while the other underestimated them. The fracture results were given in terms of probability of failure vs. strain for biaxially loaded specimens of the size used in the standard tensile tests (0.07 cubic inches). Limited data were given on the effect of biaxiality on fracture, but no correlation with theory was attempted.

1

The primary objective of the present paper is to show how the uniaxial stress-strain data and uniaxial fracture statistics can be generalized with the aid of theory to stress analyze the rotating disks and also account for the observed failure statistics. It is shown that agreement between theory and experiment is good for both types of problems.

A second objective is to investigate the applicability of weakest link theory and its associated volume effect. In one recent study[2] it was concluded that larger specimens break at a lower stress in accord with theory, but the quantitative agreement between theory and experiment left something to be desired. In another,[3] no volume effect was found. The present investigation supports weakest link theory and the implied volume effect quantitatively as well as qualitatively.

EXPERIMENTAL DATA

The experimental set-up, procedure, and data reduction techniques are described in detail in Reference 1. Briefly, the ATJS disks were 0.4" thick and 4" in diameter, and were cut so that the material was isotropic and exhibited with-grain properties in the plane of the disk. The with-grain stress-strain relation is shown in Fig. 1. The average specific gravity of the graphite was 1.83, and the Poisson coefficient was 0.1.

At the center of the rotating disk the radial strain ϵ_r is equal to the circumferential strain ϵ_θ. Figure 2 shows how this strain varies with speed of rotation for an elastic disk and also for disks obeying the Weiler-OASIS and Jones-Nelson constitutive relations. Also shown is the range of measured values of this strain at the time of disk fracture. The experimental data exhibit considerable scatter as a result of variations in material properties, but one theoretical calculation almost always underestimated the strain, while the other nearly always overestimated it.
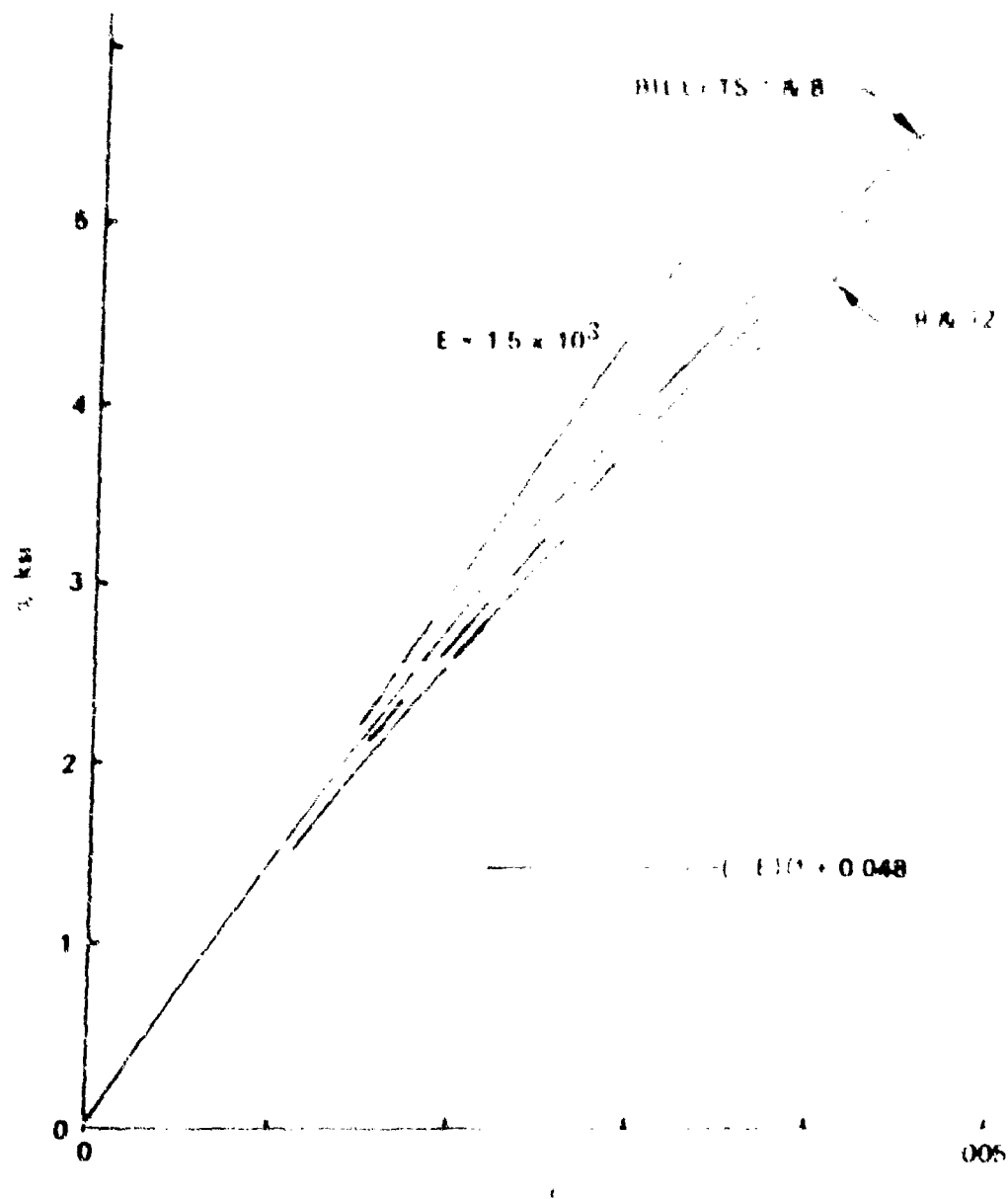
Figure 1   Median Stress Strain Curves for ATJ S Billets in With Grain
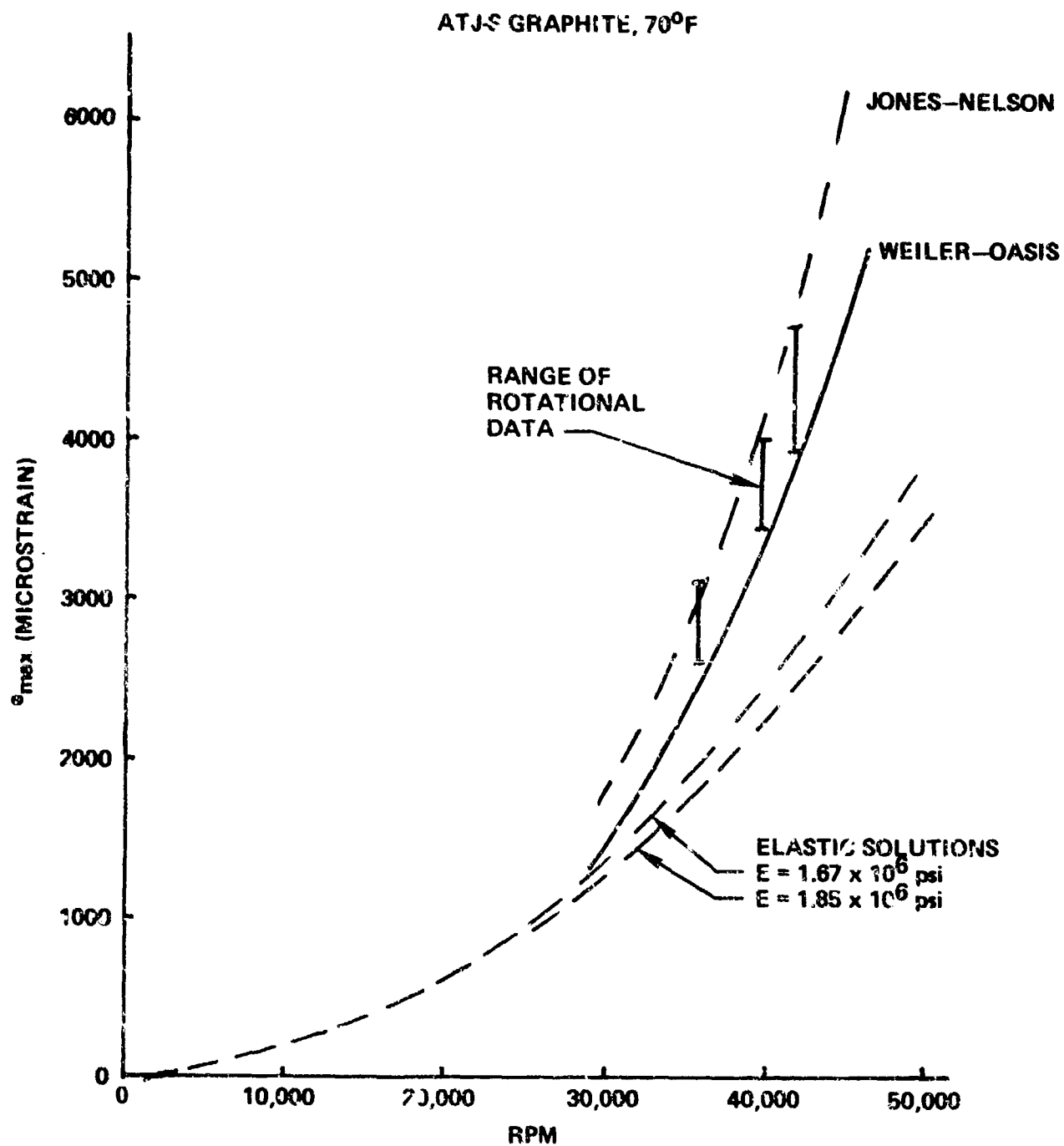Tension at Room Temperature (Adapted from Ref 1)

1

Figure 2. Measured and Predicted Maximum Strains in Disks (Taken from Ref. 1)

Table 1 summarizes the fracture data. For each specimen the rotation speed at failure is listed, together with the center strain and the maximum principal strain at the location of the crack causing the failure, as calculated by a method described in Reference 1. These data were processed by a method also discussed in Reference 1 to give the probability of failure vs. maximum principal strain for specimens having a volume of 0.07 cubic inches. By considering separately the cases of fractures originating at radii less than 0.65", 1.1", and 2" respectively, an approximate measure of the effect of biaxiality was obtained. The biaxial results are displayed in Fig. 3. Also shown are uniaxial data obtained from standard test specimens.

STRESS ANALYSIS OF DISK

The stress analysis of a loaded body requires the simultaneous satisfaction of the equations of equilibrium, compatibility, and the constitutive equations for the material. Because of the radial symmetry of the problem under consideration, derivatives in the tangential direction vanish and the equations of stress equilibrium reduce to the single equation

$$\frac{d}{dr} (r\sigma_r) = \sigma_\theta - \frac{\rho\omega^2 r^2}{g} \tag{1}$$

with the boundary condition $\sigma_r(2) = 0$. ρ is material density, and ω is angular speed in radians/second. The equations of compatibility also reduce to a single equation;

$$\frac{d}{dr} (r\varepsilon_\theta) = \varepsilon_r \tag{2}$$

The above two equations in four unknowns can be solved when we add two stress-strain equations involving the same unknowns.

In Reference 4 a stress-strain relation for ATJ-S graphite was proposed that becomes in the biaxial case

TABLE 1

BIAXIAL DISK DATA ORDERED BY INCREASING MAXIMUM PRINCIPAL STRAIN AT FAILURE

Calculated Strain at Fracture e_x (Microstrain)	Specimen No.	Fracture Measurements		
		e_{max}	RPM	Location x (inch)
1,824	12R4-3	2,280	33,000	1.5
2,558	1R3-1	3,100	37,000	1.4
2,616	12R4-4	2,930	37,000	1.3
2,648	1R3-2	2,750	36,000	0.65
2,680	1R1-2	2,680	36,500	0
2,964	8R4-3	3,000	38,200	0.4
3,000	1R3-5	3,100	38,200	0.6
3,072	1R1-4	3,200	36,400	0 7
3,115	8R2-2	3,300	38,500	1.1
3,119	1R1-3	3,300	39,000	0 8
3,136	12R2-5	3,200	37,600	0.5
3,137	12R4-2	3,150	35,700	0.2
3,179	1R3-3	3,400	40,300	0.85
3,214	9R3-4	3,260	37,600	0.4
3,230	12R4-1	3,550	39,400	1.0
3,232	8R2-4	3,420	40,000	0 8
3,283	12R2-4	3,350	39,000	0 5
3,286	9R3-3	3,320	38,800	0 3
3,293	8R4-4	3,360	39,700	0 5
3,332	9R3-2	3,400	40,400	0.5
3,360	12R2-1	3,680	38,400	0.25
3,398	8R4-2	3,540	40,800	0.7
3,399	9R3-5	3,530	38,700	0 65
3,445	9R1-4	3,480	40,000	0 35
3,446	9R1-2	3,460	39,600	0 2
3,458	1R1-5	3,500	40,400	0.4
3,471	8R2-3	3,900	40,400	1.1
3,540	9R1-5	3,410	41,000	0 6
3,563	12R2-3	3,700	40,400	0.65
3,577	8R2-5	3,650	38,800	0.5
3,600	9R1-3	3,750	40,700	0 7
3,626	9R1-1	3,700	40,400	0.5
3,705	8R4-1	3,900	42,400	0.75
3,707	1R1-1	4,030	41,000	0 95
3,952	9R3-1	4,250	43,000	0.9
3,961	12R4-5	4,170	42,300	0.75
3,991	8R2-1	4,040	41,000	0.40
4,051	1R3-4	4,220	40,400	0.7
4,413	12R2-2	4,550	42,000	0

6

ATJ-S GRAPHITE

DATA FROM 39 ROTATING DISKS, FOR V = 0.07 IN³

SYMBOL	MATERIAL CONSIDERED	MINIMUM BIAXIAL STRESS RATIO
○	ENTIRE DISK, R=2"	0
●	VOLUME WITHIN 1.1" R.	0.7 → 0.85
△	VOLUME WITHIN 0.65" R.	0.9 → 0.95

ESTIMATED PROBABILITY OF FRACTURE, PERCENT

DATA FROM 32 STANDARD TENSILE TESTS

NOMINAL BIAXIAL STRESS RATIO

$\sigma_R/\sigma_\theta =$

~ 0.95

~ 0.80

< 0.70

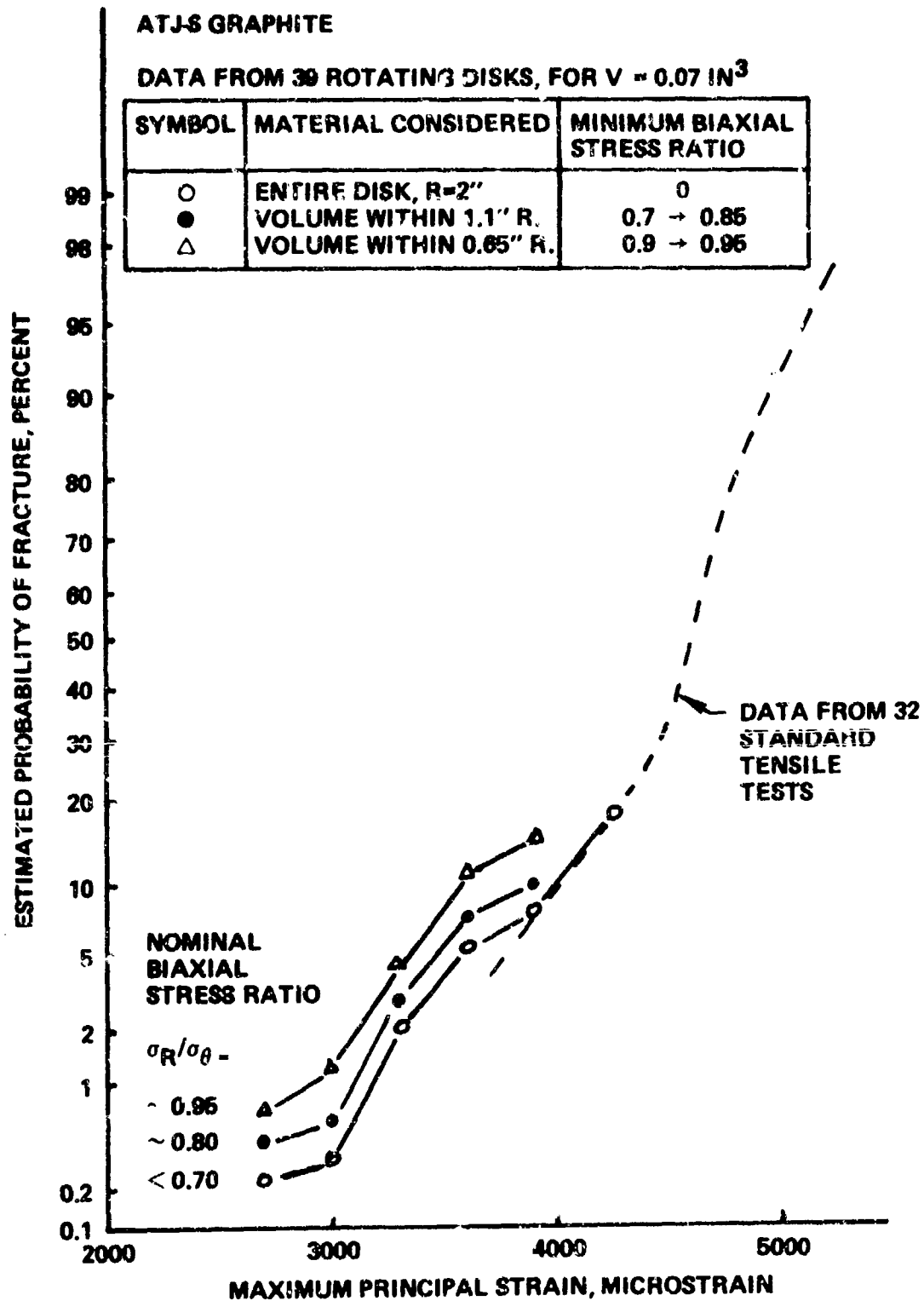MAXIMUM PRINCIPAL STRAIN, MICROSTRAIN

Figure 3. Ogives for Failure Strain, Calculated for a Volume of 0.07 Cubic Inch
(Adapted from Ref. 1).

7

$$\epsilon_r = \frac{\sigma_r}{E}(1 + F) - \frac{0.1}{E}\sigma_\theta \qquad (3)$$

$$\epsilon_\theta = -\frac{0.1}{E}\sigma_r + \frac{\sigma_\theta}{E}(1 + F) \qquad (\;)$$

where

$$F = K_1 \sqrt{\frac{\sigma_r^2 + \sigma_\theta^2}{(\sigma_r^0)^2} - 1} \qquad (5)$$

In Eq. (5) σ_r^0 is the elastic limit stress in the with-grain direction and K_1 is a constant to be adjusted to give good agreement with the uniaxial stress strain curve near the fracture point.

The stress-strain curves shown in Fig. 1 do not exhibit an elastic limit, so for simplicity of analysis it is assumed equal to zero. As a result, Eq. (5) becomes

$$F = \frac{K_1}{\sigma_r^0}\sqrt{\sigma_r^2 + \sigma_\theta^2 - (\sigma_r^0)^2}$$

$$= K_2 \sqrt{\sigma_r^2 + \sigma_\theta^2} \qquad (6)$$

when σ_r^0 approaches zero. The choice $E = 1.5 \times 10^3$ ksi and $K_2 = 0.048$ (ksi)$^{-1}$ leads to good agreement with the uniaxial stress strain curve, as is apparent from Fig. 1. Thus our choice of biaxial stress-strain relations becomes

$$\epsilon_r = \frac{\sigma_r}{1500}\left(1 + 0.048\sqrt{\sigma_\theta^2 + \sigma_r^2}\right) - 6.7 \times 10^{-5}\,\sigma_\theta \qquad (7)$$

$$\epsilon_\theta = -6.7 \times 10^{-5}\,\sigma_r + \frac{\sigma_\theta}{1500}\left(1 + 0.048\sqrt{\sigma_\theta^2 + \sigma_r^2}\right) \qquad (8)$$

In the above equations stresses are expressed in ksi.

In Fig. 4 the equibiaxial stress-strain behavior implied by equations (7) and (8) is compared with the uniaxial behavior. For comparison, the corresponding curves as calculated in the Weiler-OASIS and Jones-Nelson approaches
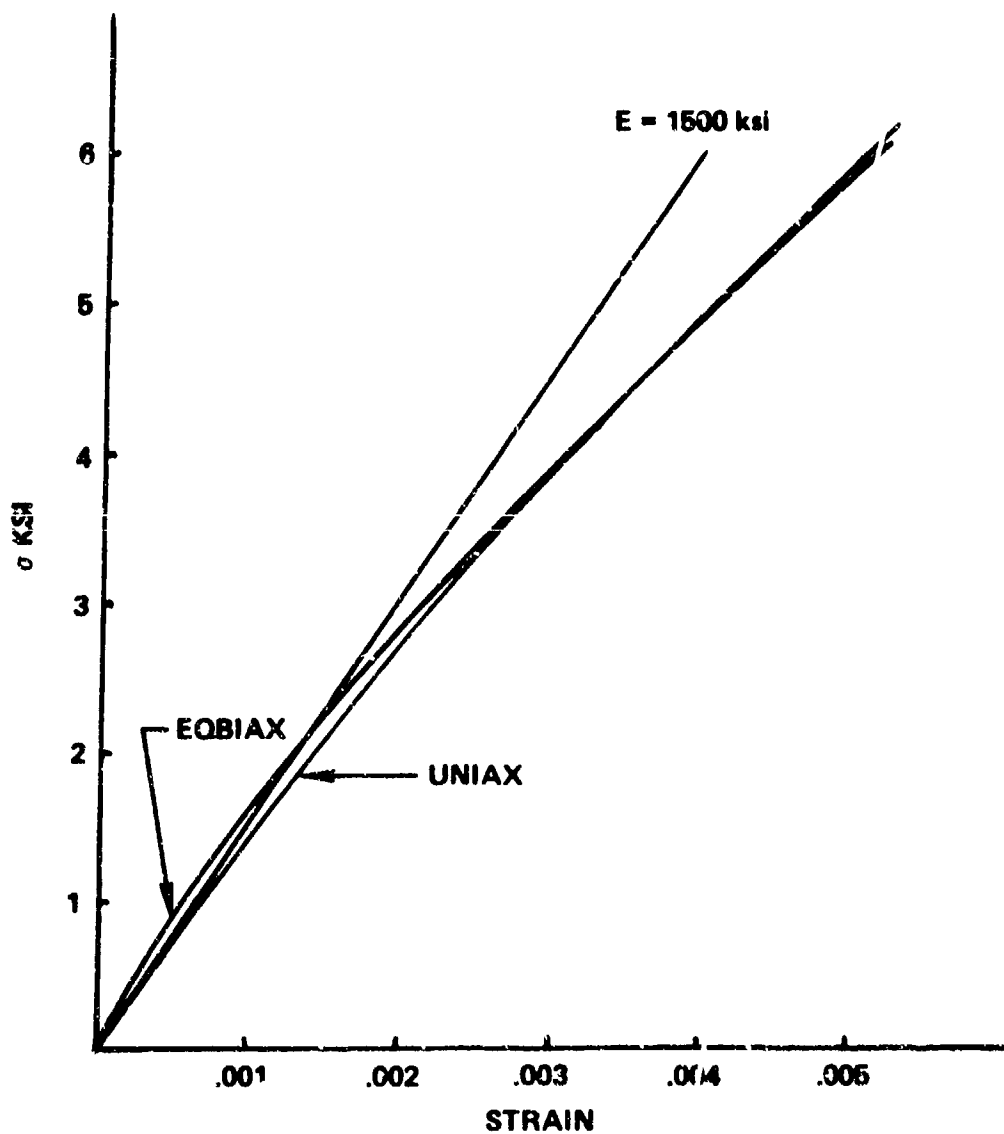
8

Figure 4. Comparison of Uniaxial and Equibiaxial With-Grain Stress Strain Response of ATJS Graphite, Using Theory of Reference 4.

are given in Fig. 5. Whereas in the Weiler-OASIS treatment the equibiax curve is generally higher than the uniaxial and in the Jones-Nelson treatment it is substantially lower, Eqs. (7) and (8) imply the two curves are very close together, especially at the stresses at which most of the fractures occurred.

Equations (1) and (2), (7) and (8) were solved simultaneously by iteration for a series of values of ω, and the results are given in Table 2. The way in which stress and strain vary with radius is shown in Figs. 6 and 7 respectively. Figure 8 shows the manner in which the maximum strain varies with speed of rotation and compares the result with the experimental data from Reference 1. The present calculation agrees significantly better with the data than the calculations based on the Weiler-OASIS and Jones-Nelson approaches.

FRACTURE STATISTICS

Statistical theories of fracture are usually formulated in terms of stresses. The simplest treatment involves the use of Weibull's 2-parameter form[5] which assumes for the probability of fracture in uniform uniaxial tension

$$P_f = 1 - \exp[-Vk_o\sigma^m] \tag{9}$$

In this equation V is the volume, and the parameters k_o and m are chosen for optimum fit to the experimental data. Figure 3 contains experimental data on probability of fracture of standard tensile test specimens as a function of strain, but the data apply to higher strains than those at which the majority of disk fractures occurred.

There is no reliable way of extrapolating the standard tensile specimen data to the strain levels at which most of the disks fractured, expecially since the data as presented in Fig. 3 do not conform well to any of the
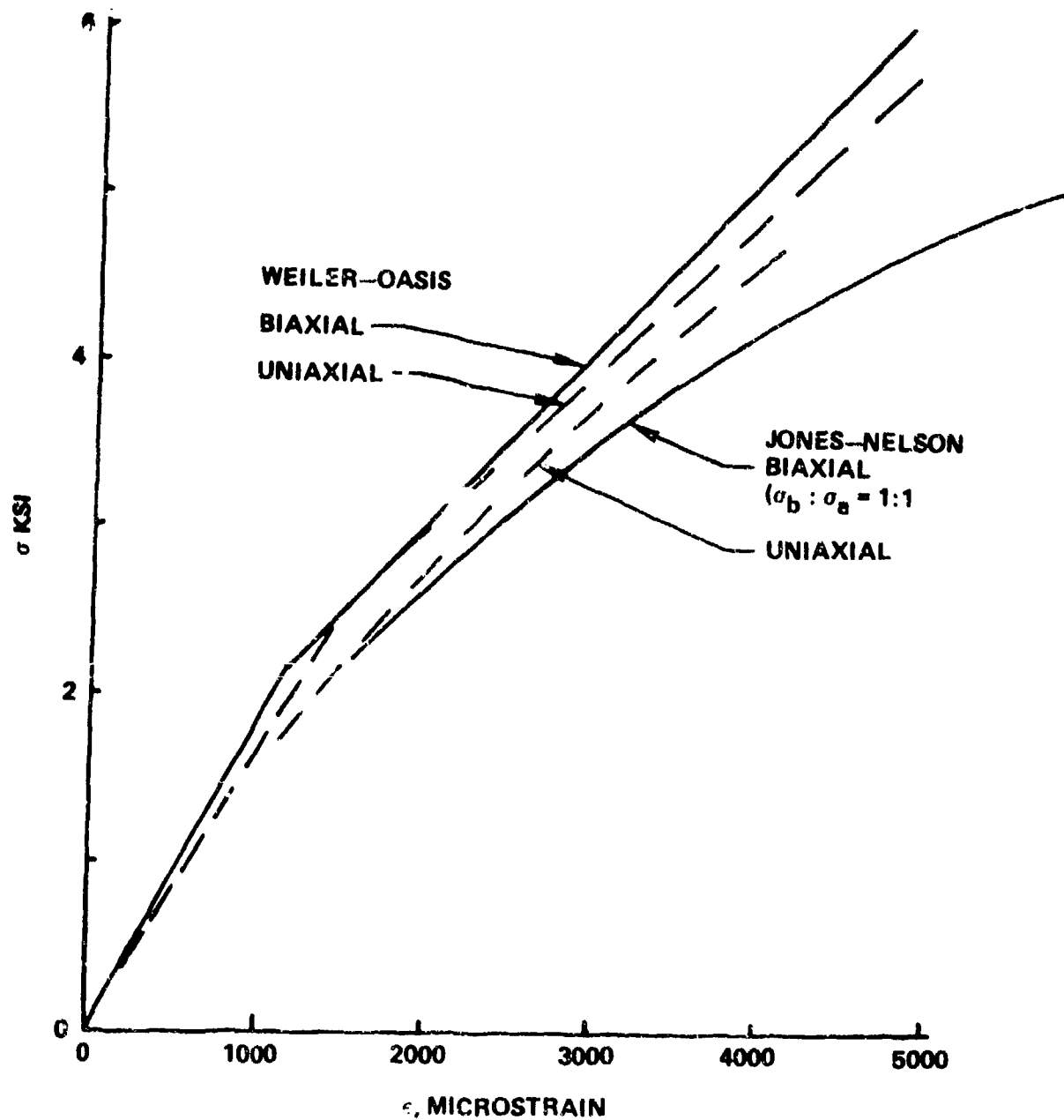
Figure 5. Predictions of With-Grain Stress-Strain Response in Equal (1:1) Biaxial Tension, ATJ-S (Taken from Ref 1).

TABLE 2

STRESSES AND STRAINS IN
ROTATING ATJS DISKS

W(Rad./sec.)

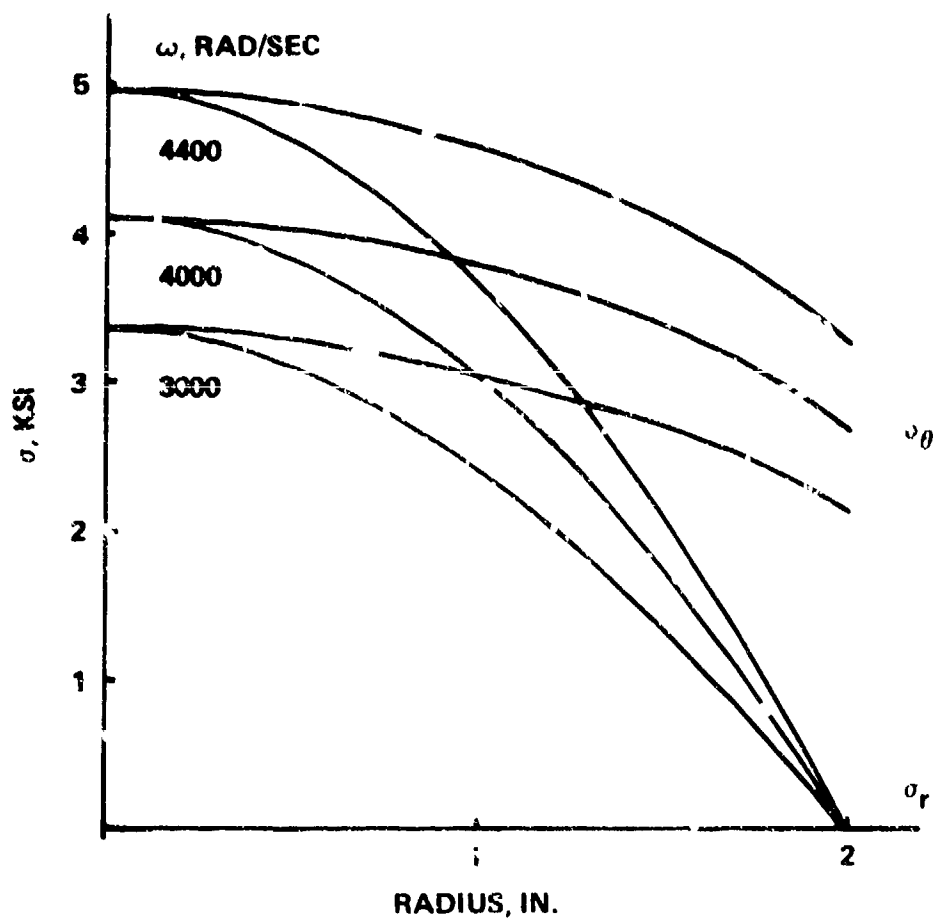|	R	ETHETA	ER	SR	STHETA
	.01	2.5124E-03	2.5124E-03	3.3452E+00	3.3452E+00
	.20	2.4735E-03	2.4475E-03	3.3113E+00	3.3285E+00
	.40	2.4673E-03	2.3031E-03	3.2115E+00	3.2357E+00
	.60	2.4161E-03	2.2405E-03	3.0585E+00	3.2390E+00
3600	.80	2.3665E-03	2.0472E-03	3.8000E+00	3.1845E+00
	1.00	2.2560E-03	1.7737E-03	2.4951E+00	3.0547E+00
	1.20	2.1519E-03	1.4655E-03	2.1239E+00	2.9275E+00
	1.40	2.0543E-03	1.1131E-03	1.6557E+00	2.5922E+00
	1.60	1.9653E-03	7.2097E-04	1.1804E+00	2.5922E+00
	1.80	1.7310E-03	3.1329E-06	6.3424E-01	2.7815E+00
	2.00	1.6692E-03	-1.4297E-04	0.	2.133E+00
	.01	2.8537E-03	2.8537E-03	3.7164E+00	3.7164E+00
	.20	2.8366E-03	2.8194E-03	3.6795E+00	3.6965E+00
	.40	2.8019E-03	2.5169E-03	3.5678E+00	3.6626E+00
	.60	2.7474E-03	2.5439E-03	3.3763E+00	3.6012E+00
3800	.80	2.6619E-03	2.3063E-03	3.1115E+00	3.5139E+00
	1.00	2.5535E-03	2.0103E-03	2.7731E+00	3.4014E+00
	1.20	2.4373E-03	1.6894E-03	2.3606E+00	3.2627E+00
	1.40	2.3455E-03	1.2588E-03	1.8739E+00	3.0955E+00
	1.60	2.1394E-03	8.1436E-04	1.3124E+00	2.8972E+00
	1.80	1.9654E-03	3.5779E-04	2.0522E-01	2.6601E+00
	2.00	1.7786E-03	-1.6033E-04	0.	2.3930E+00
	.01	3.2253E-03	3.2253E-03	4.1061E+00	4.1061E+00
	.20	3.2058E-03	3.1862E-03	4.0552E+00	4.0855E+00
	.40	3.1663E-03	3.0503E-03	3.9417E+00	4.0478E+00
	.60	3.0973E-03	2.8717E-03	3.7406E+00	3.9510E+00
4000	.80	3.0073E-03	2.6029E-03	3.4364E+00	3.8406E+00
	1.00	2.8910E-03	2.2869E-03	3.0646E+00	3.7666E+00
	1.20	2.7524E-03	1.8694E-03	2.6090E+00	3.6167E+00
	1.40	2.6329E-03	1.4166E-03	2.0713E+00	3.4366E+00
	1.60	2.4176E-03	9.1536E-04	1.4509E+00	3.2205E+00
	1.80	2.2142E-03	3.9740E-04	7.7969E-01	2.9641E+00
	2.00	2.0104E-03	-1.7937E-04	0.	2.6601E+00
	.01	3.6293E-03	3.6293E-03	4.5143E+00	4.5143E+00
	.20	3.6071E-03	3.5849E-03	4.4693E+00	4.4930E+00
	.40	3.5622E-03	3.4521E-03	4.3734E+00	4.4515E+00
	.60	3.4851E-03	3.2284E-03	4.1314E+00	4.3805E+00
4200	.80	3.3425E-03	3.0243E-03	3.7404E+00	4.2805E+00
	1.00	3.2513E-03	2.5448E-03	3.1606E+00	4.1505E+00
	1.20	3.0947E-03	2.0646E-03	2.5689E+00	3.9804E+00
	1.40	2.9147E-03	1.5869E-03	2.2774E+00	3.7047E+00
	1.60	2.7124E-03	1.0243E-03	1.5956E+00	3.5622E+00
	1.80	2.4927E-03	4.4657E-04	8.5762E-01	3.2867E+00
	2.00	2.2558E-03	-1.9949E-04	0.	2.9625E+00
	.01	4.0675E-03	4.0675E-03	4.9409E+00	4.9409E+00
	.20	4.0425E-03	4.0174E-03	4.8917E+00	4.9180E+00
	.40	3.9019E-03	3.8673E-03	4.7427E+00	4.8735E+00
	.60	3.9032E-03	3.6146E-03	4.4487E+00	4.7985E+00
4400	.80	3.7436E-03	3.2721E-03	4.1374E+00	4.6916E+00
	1.00	3.6619E-03	2.8451E-03	3.6940E+00	4.5530E+00
	1.20	3.4690E-03	2.3616E-03	3.1501E+00	4.3809E+00
	1.40	3.2613E-03	1.7704E-03	2.4933E+00	4.1724E+00
	1.60	3.0170E-03	1.1417E-03	1.7467E+00	3.9325E+00
	1.80	2.7002E-03	4.9657E-04	9.3497E-01	3.6277E+00
	2.00	2.5251E-03	-2.1931E-04	0.	3.2375E+00

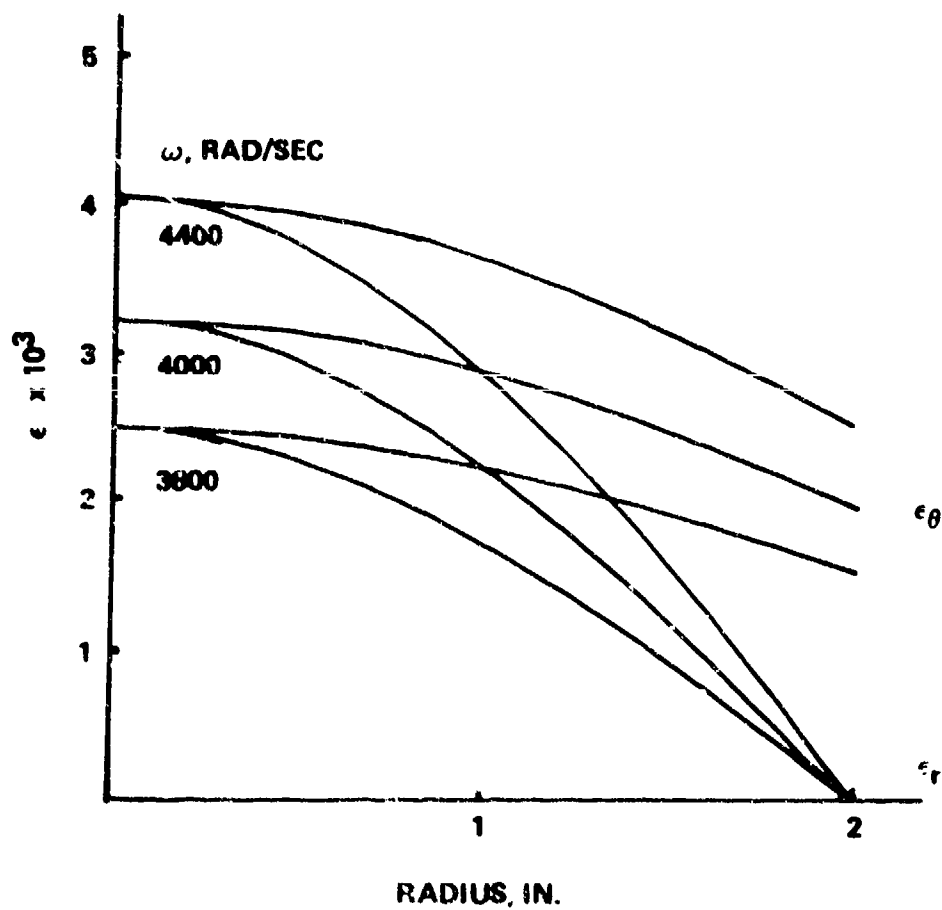Figure 6. Computed Stress Distribution in Rotating ATJS Disks.

13

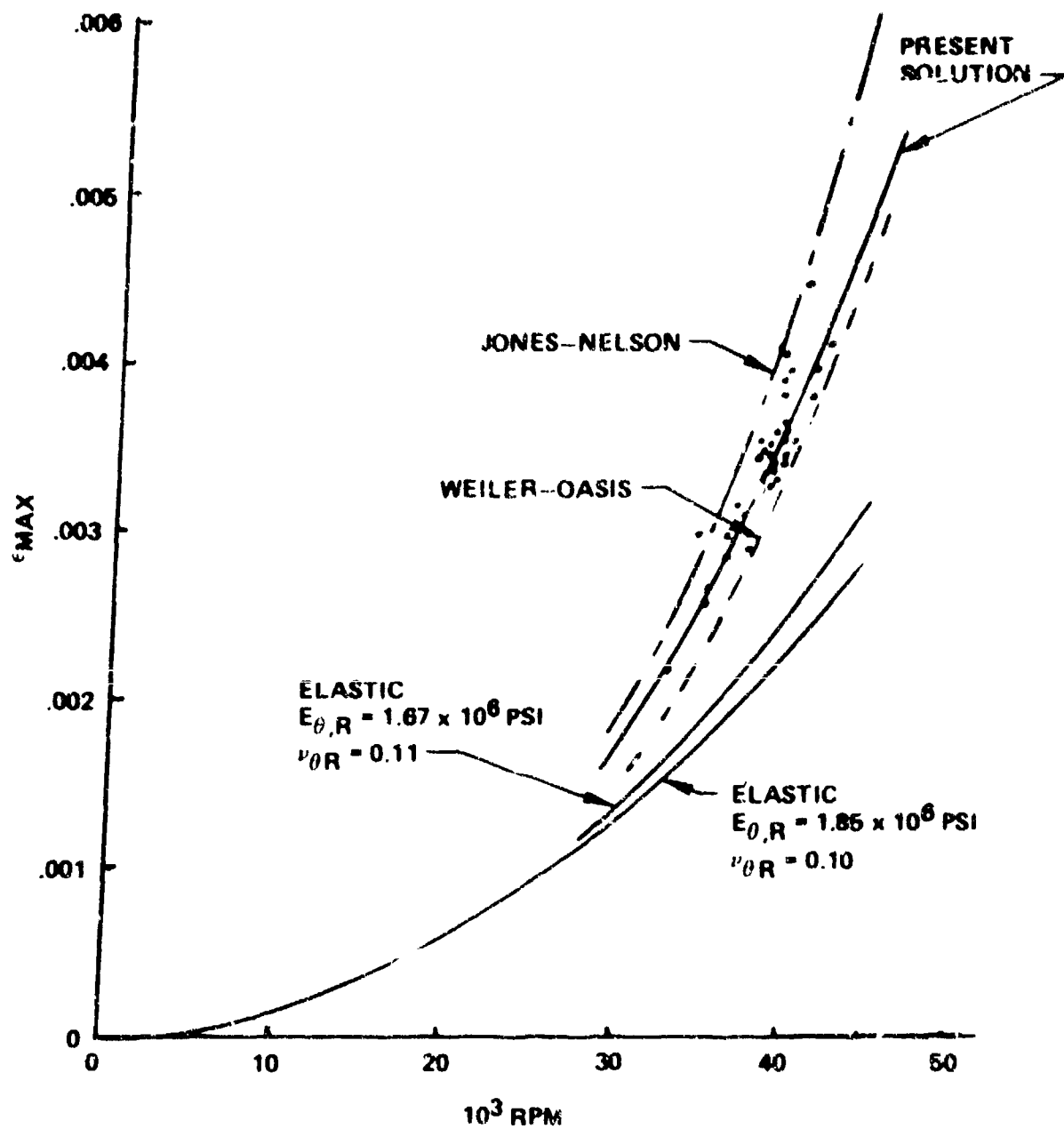Figure 7.   Computed Strain Distribution in Rotating ATJS Disks.

Figure 8   Maximum Strains Predicted in Four-Inch Diameter ATJ-S Disks Compared To Jortner's Test Data.

15

theoretical formulations in general use. Accordingly, we shall employ theory to deduce from the disk fracture data what the uniaxial fracture statistics in the desired stress range must be. The procedure followed here is to assume the uniaxial statistics obey Eq. (9) and then apply the statistical theory for biaxial stresses to determine what values of m and k_o lead to the observed disk fracture statistics.

When it is assumed that the uniaxial tensile fracture statistics obey Eq. (9) and that fracture is determined solely by the component of stress normal to the crack plane, the biaxial tensile statistics become (Ref. 6)

$$P_f = 1 - \exp\left[- Vk\left(\frac{\sigma_2}{\sigma_1}, m\right)\sigma_1^m \right] \tag{10}$$

where σ_1 and σ_2 are the principal stresses with $\sigma_2 \leq \sigma_1$ and

$$\frac{k\left(\frac{\sigma_2}{\sigma_1}, m\right)}{k_o} = \frac{(m!)^2}{(2m)!} \sum_{i=0}^{m} \frac{(2i)![2(m-i)]!}{[i!(m-i)!]^2} \left(\frac{\sigma_2}{\sigma_1}\right)^i \tag{11}$$

Table 3 lists the values of this ratio for a number of values of m and σ_2/σ_1, and Fig. 9 contains curves for selected values of m.

The above considerations can be used to calculate the probability of survival of the rotating disks of Reference 1 as a function of the speed of rotation. The applicable equation is

$$P_f(\omega) = 1 - \exp\left[- \int k\left(\frac{\sigma_r}{\sigma_\theta}, m\right) \sigma_\theta^m \, dV \right] \tag{12}$$

$$= 1 - \exp\left[- k_o \, \sigma_{max}^m \, C_m \right]$$

where

$$C_m \equiv \int_0^2 2\pi r t \, \frac{k\left(\frac{\sigma_r}{\sigma_o}, m\right)}{k_o} \left(\frac{\sigma_\theta}{\sigma_{max}}\right)^m \, dr \tag{13}$$

Table 3

Values of $k(\sigma_r/\sigma_\theta)/k_0$

$m \rightarrow$	2	3	5	7	1?	20
(σ_r/σ_θ) ↓ 0	1.0	1.0	1.0	1.0	1.0	1.0
0.2	1.173	1.153	1.135	1.129	1.124	1.122
0.4	1.427	1.400	1.353	1.331	1.311	1.302
0.6	1.760	1.793	1.758	1.710	1.646	1.615
0.8	2.173	2.377	2.549	2.584	2.017	2.399
0.9	2.410	2.756	3.188	3.430	3.664	3.653
0.95	2.536	2.970	3.593	4.026	4.678	5.113
0.98	2.614	3.106	3.867	4.455	5.518	6.588
1.0	2.667	3.200	4.063	4.774	6.204	7.975
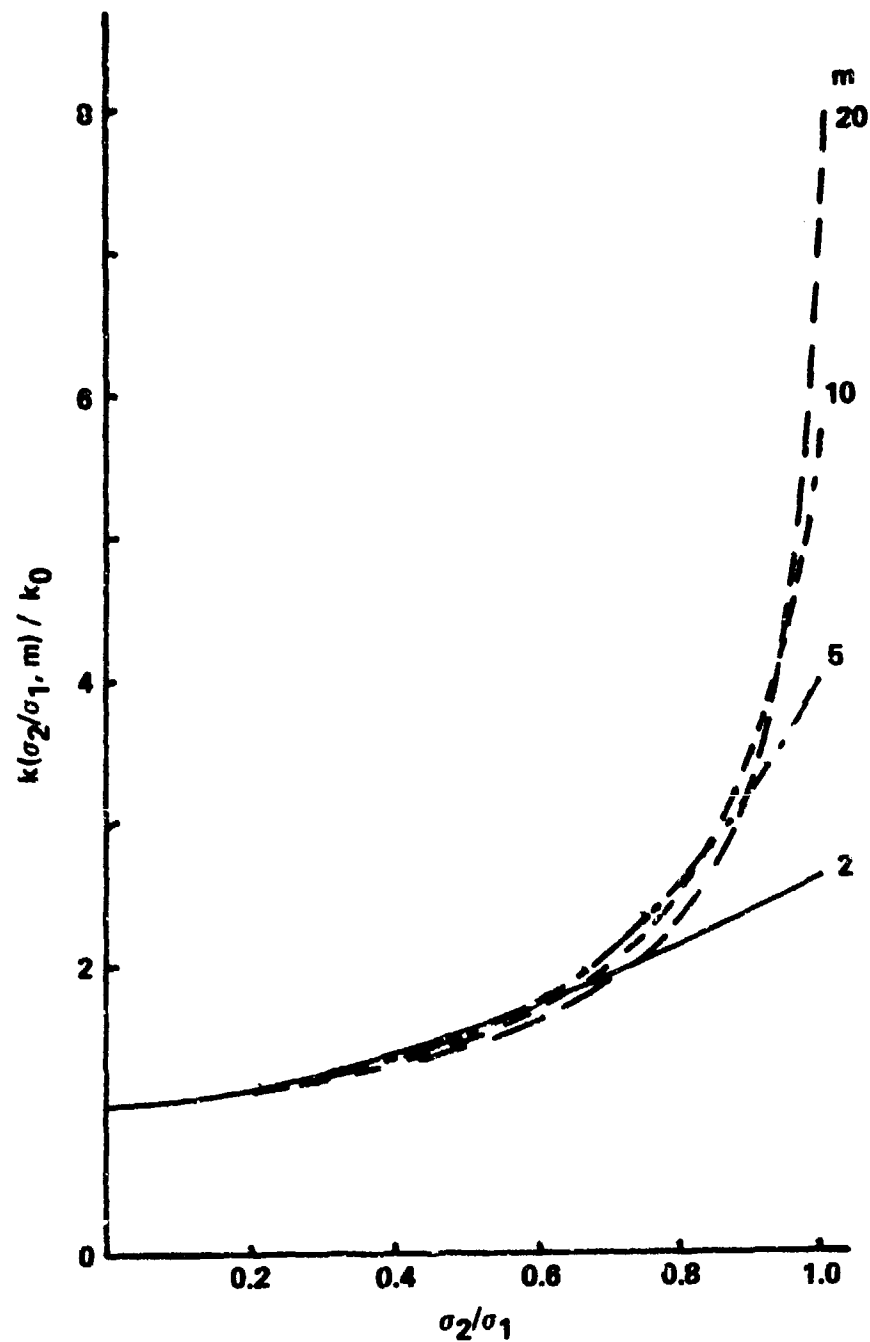
Figure 3. Variation of k With Biaxiality.

The k ratio and the σ ratio appearing in the integral in Eq. (13) are both virtually independent of the rate of rotation. Accordingly we evaluate the integral after m is determined, using the stress ratios for the rotation speed in Table 2 coming closest to a failure probability of 50%, i.e., $\omega = 4200$ rad./sec.

The experimental data in Table 1 can be used to determine P_f as a function of the rate of rotation. A plot of failure probability vs. rotation speed is given in Fig. 10. We find the values of m and $C_m k_o$ to fit these data as follows. For two selected values of ω for which σ_{max} appears in Table 2 we require that Eq. (12) gives the experimental results of Fig. 10. It then follows that

$$\frac{\ln[1-P_f(\omega_1)]}{\ln[1-P_f(\omega_2)]} = \left[\frac{\sigma_{max}(\omega_1)}{\sigma_{max}(\omega_2)}\right]^m \tag{14}$$

Assuming P_f at 3800 rad./sec. is 0.1 and P_f at 4200 is 0.64, we obtain $m = 12$. Then using Eq. (12) we find that $k_o C_m = 1.43 \times 10^{-8}$. $P_f(\omega)$ is now completely defined, and is plotted in Fig. 10.

To find k_o we must evaluate C_m. This can be done as follows. Figure 11 shows σ_o/σ_{max} as a function of r for $\omega = 4200$ rad/sec. To a close approximation the ratio is given by

$$\frac{\sigma_\theta(r)}{\sigma_{max}} = 1 - 0.086 \ r^2 \tag{15}$$

Figure 12a shows σ_r/σ_θ as a function of r. Combining this result with the data in Table 2 for $m = 12$, we obtain the results shown in Fig. 12b for $k\left(\frac{\sigma_r}{\sigma_\theta}, 12\right)/k_o$. Evaluating the integral in Eq. (13) with the aid of Eq. (15) and Fig. 12 we obtain $C_m = 3.4$, from which it follows that k_o is 4.2×10^{-9}. Thus we conclude that in the stress range within which disk fractures occurred, simple tensile fracture obeys the equation
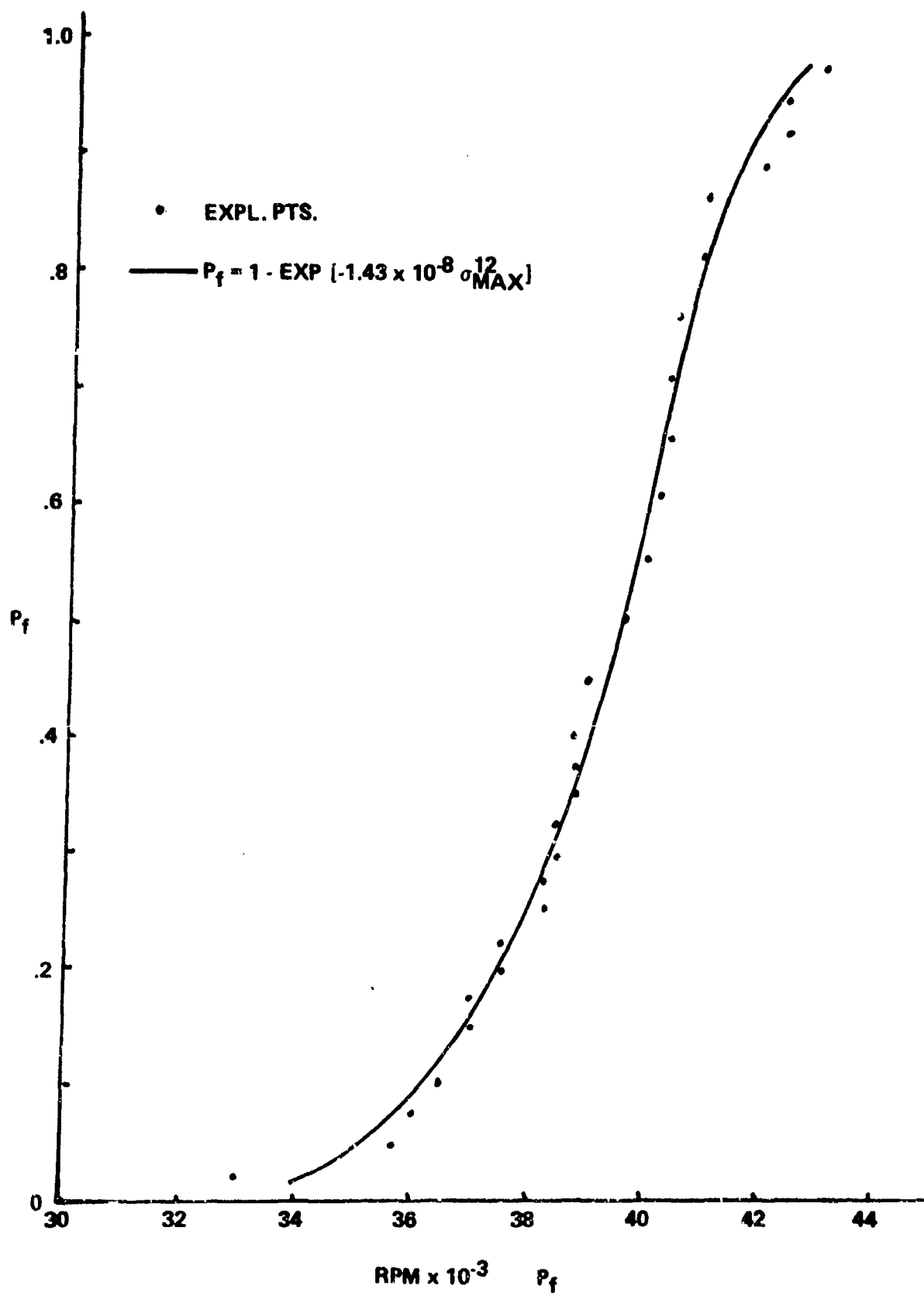
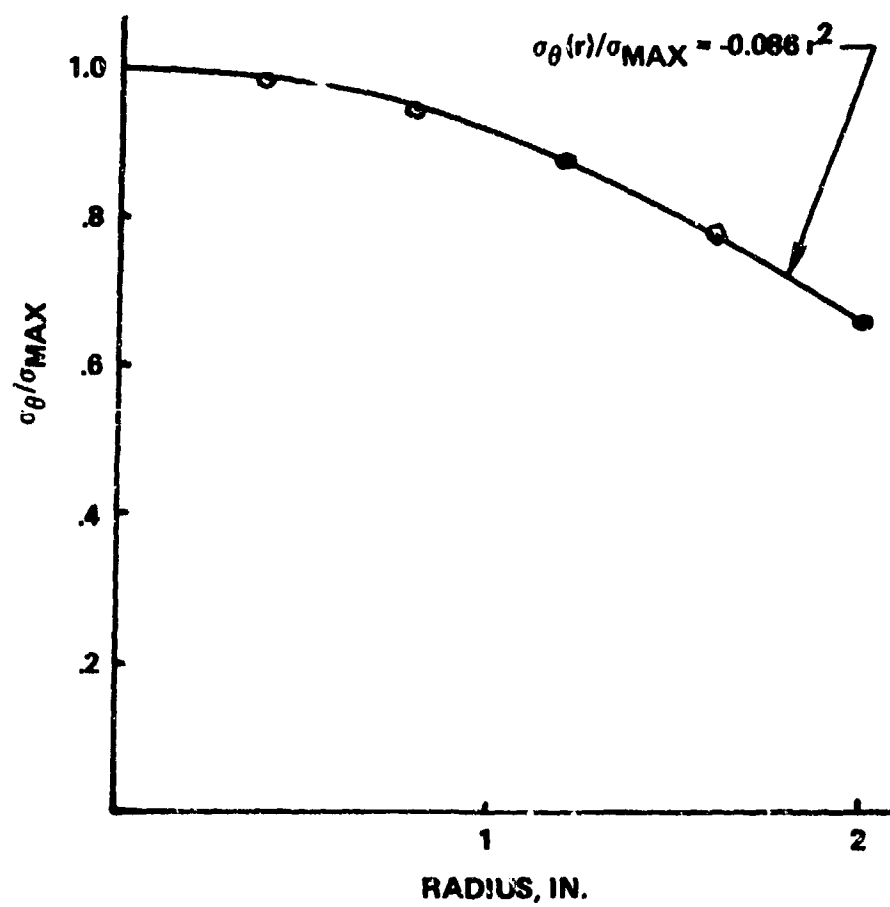Figure 10. Probability of Failure of Spinning ATJS Graphite Disks.

Figure 11. Comparison Between Computed Points and Analytical Approximation
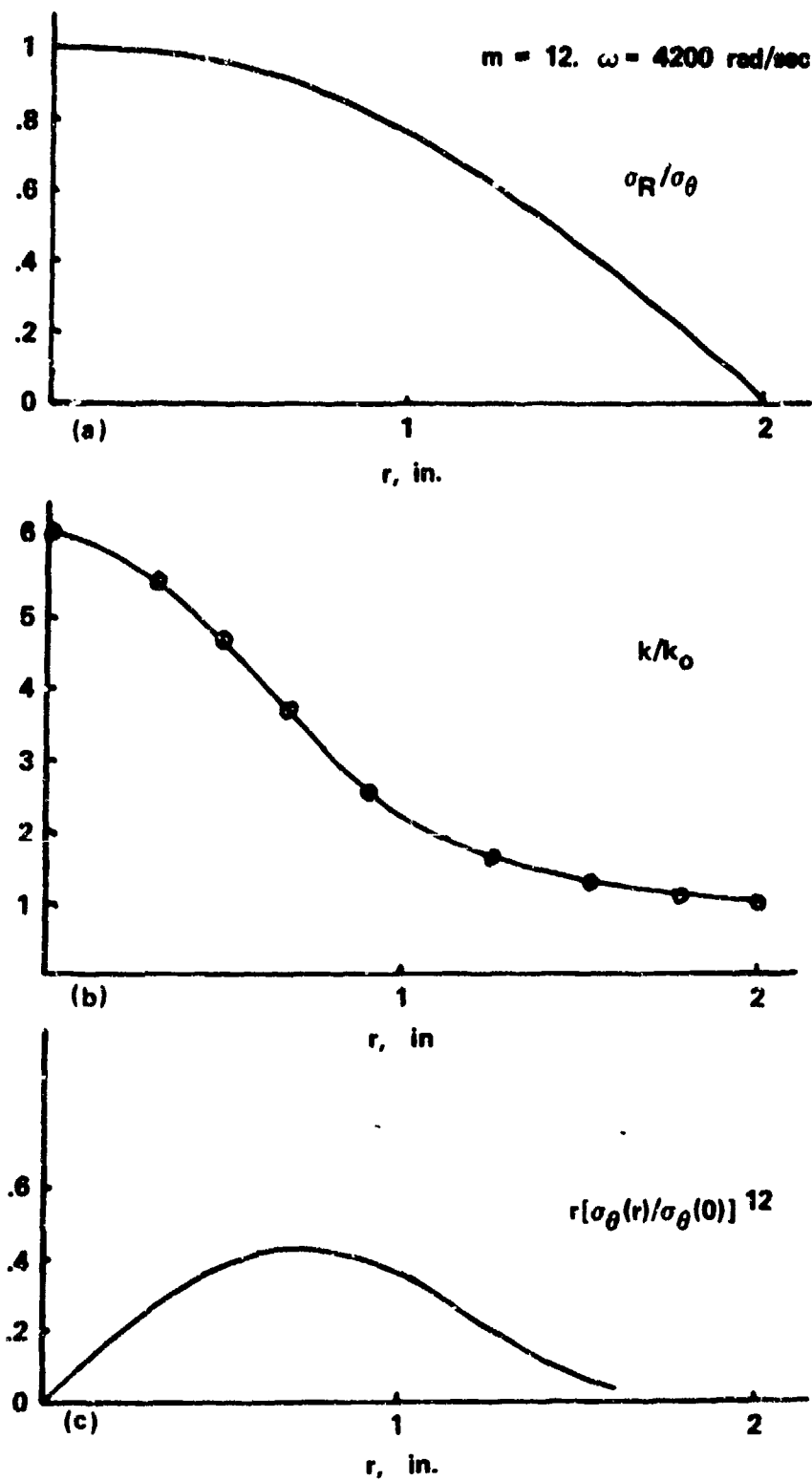At $\omega = 4200$ rad./sec.

$m = 12.$ $\omega = 4200$ rad/sec

(a) σ_R/σ_θ

(b) k/k_o

(c) $r[\sigma_\theta(r)/\sigma_\theta(0)]^{12}$

Figure 12. Theoretical Analysis of Spinning ATJS Graphite Disks.

22

$$P_f = 1 - \exp\left[-V\, 4.2 \times 10^{-9}\, \sigma^{12}\right] \tag{16}$$

Before proceeding further it is appropriate to examine the compatibility of the result just obtained with the results of standard tensile tests at a higher stress range. This is done in Fig. 13, which shows what Eq. (16) implies for specimens having a volume of 0.07 cubic inches. The stresses have been converted into strains using Eq. (8) for the uniaxial case, i.e.,

$$\epsilon = \frac{\sigma}{1500}\,(1 + 0.048\,\sigma) \tag{8'}$$

Also shown for comparison are fracture data for 20 selected standard test specimens.

The rationale for this selection is apparent from Fig. 14 which shows that the fracture origins tended to concentrate heavily at the ends of the test section (i.e. the region of uniform cross section), and even outside the test section. To compensate somewhat for this anomaly, only fractures occurring at least 0.05" inside the test section were included.

The smooth solid curve through these data looks like a reasonable extrapolation of the disk data, except for a slight vertical offset. However if the lowest point were eliminated, the resulting smooth curve would be approximately that shown dashed in the figure, which has virtually no vertical discontinuity. Thus we conclude that the disk data are compatible, within normal experimental scatter, with the data obtained using standard test specimens.

Assuming, then, that the uniaxial behavior of ATJS in the disk fracture stress range is given with satisfactory accuracy by Eq. (16), we use this relation to predict theoretically the three disk failure curves of Fig. 3. This can be done as follows:
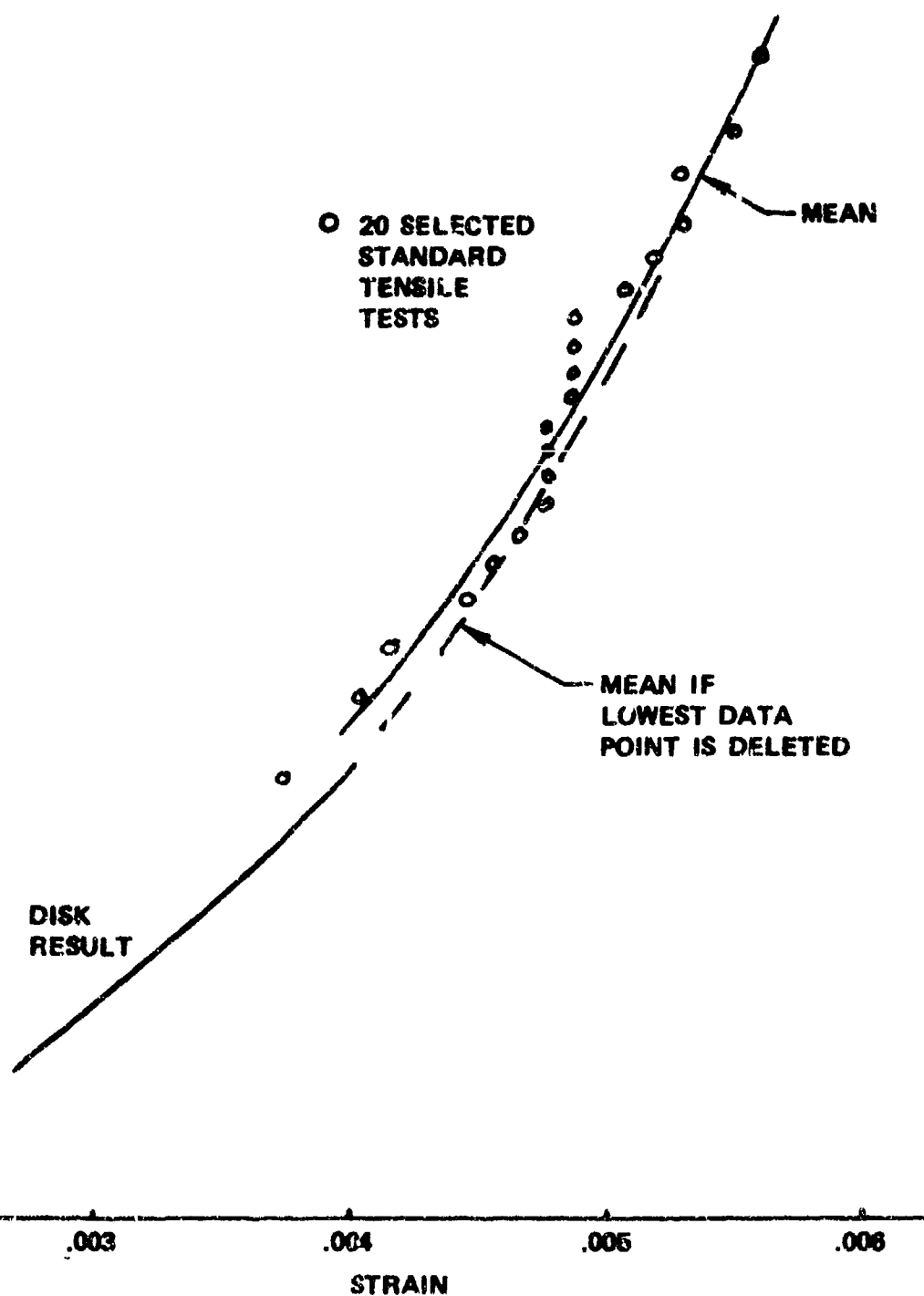
23

O 20 SELECTED STANDARD TENSILE TESTS

MEAN

MEAN IF LOWEST DATA POINT IS DELETED

DISK RESULT

.003 .004 .005 .006

STRAIN

Figure 13. Comparison of $P_f(\varepsilon)$ Data for 20 Selected Standard Tensile Specimens With $P_f(\varepsilon)$ Deduced from Disk Data.
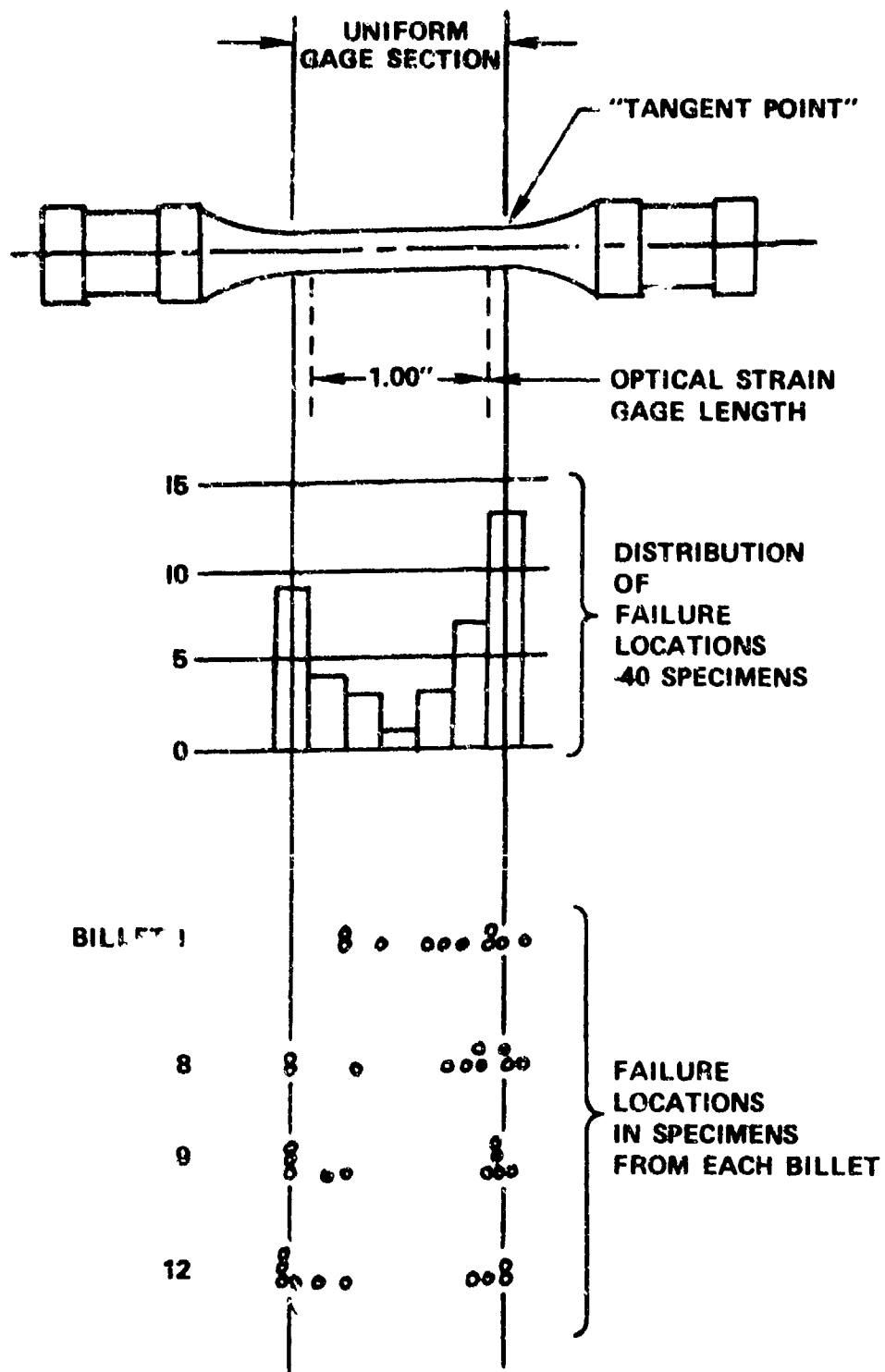
Figure 14. Fracture Locations in Standard Tensile Coupons (Taken from Ref. 1).

Since the disk data represent results for a degree of biaxiality that is averaged over the region under consideration (i.e., $r \leq r_1$) we evaluate the quantity $\bar{k}(r_1)$ that represents $k(\sigma_r/\sigma_\theta, m)$ averaged over this region. This k must obey the relation

$$\bar{k}(r_1) \int_0^{r_1} \sigma_\theta^m \, dV = \int_0^{r_1} k(\sigma_r/\sigma_\theta, m)\sigma_\theta^m \, dV \tag{17}$$

or

$$\frac{\bar{k}(r_1)}{k_o} = \frac{\int_0^{r_1} \frac{k\left(\frac{\sigma_r}{\sigma_\theta}, 12\right)}{k_o} (1-0.086 \, r^2)^{12} \, r \, dr}{\int_0^{r_1} (1-0.086 \, r^2)^{12} \, r \, dr} \tag{18}$$

The denominator can be integrated analytically by elementary means, yielding

$$\int_0^{r_1} (1-0.086 \, r^2)^{12} \, r \, dr = 0.437 \, [1-(1-0.086 \, r_1^2)^{13}] \tag{19}$$

The numerator can be evaluated numerically with the aid of Fig. 12. The result is

$$\bar{k}(0.65")/k_o = 5.1$$

$$\bar{k}(1.1")/k_o = 4.0$$

$$\bar{k}(2")/k_o = 3.4$$

Using these values of $\bar{k}$ instead of k_o in Eq. (9) and converting to strains, we obtain the curves shown in Fig. 15 for $r_1 = 0.65"$, $1.1"$, and $2"$. Comparing this result with the experimental data portrayed in Fig. 3 some significant differences are apparent (see Fig. 16). We now address the questions of what these differences are and how to resolve the discrepancies. For simplicity, attention will be limited to $r_1 = 0.65"$ and $r_1 = 2"$.
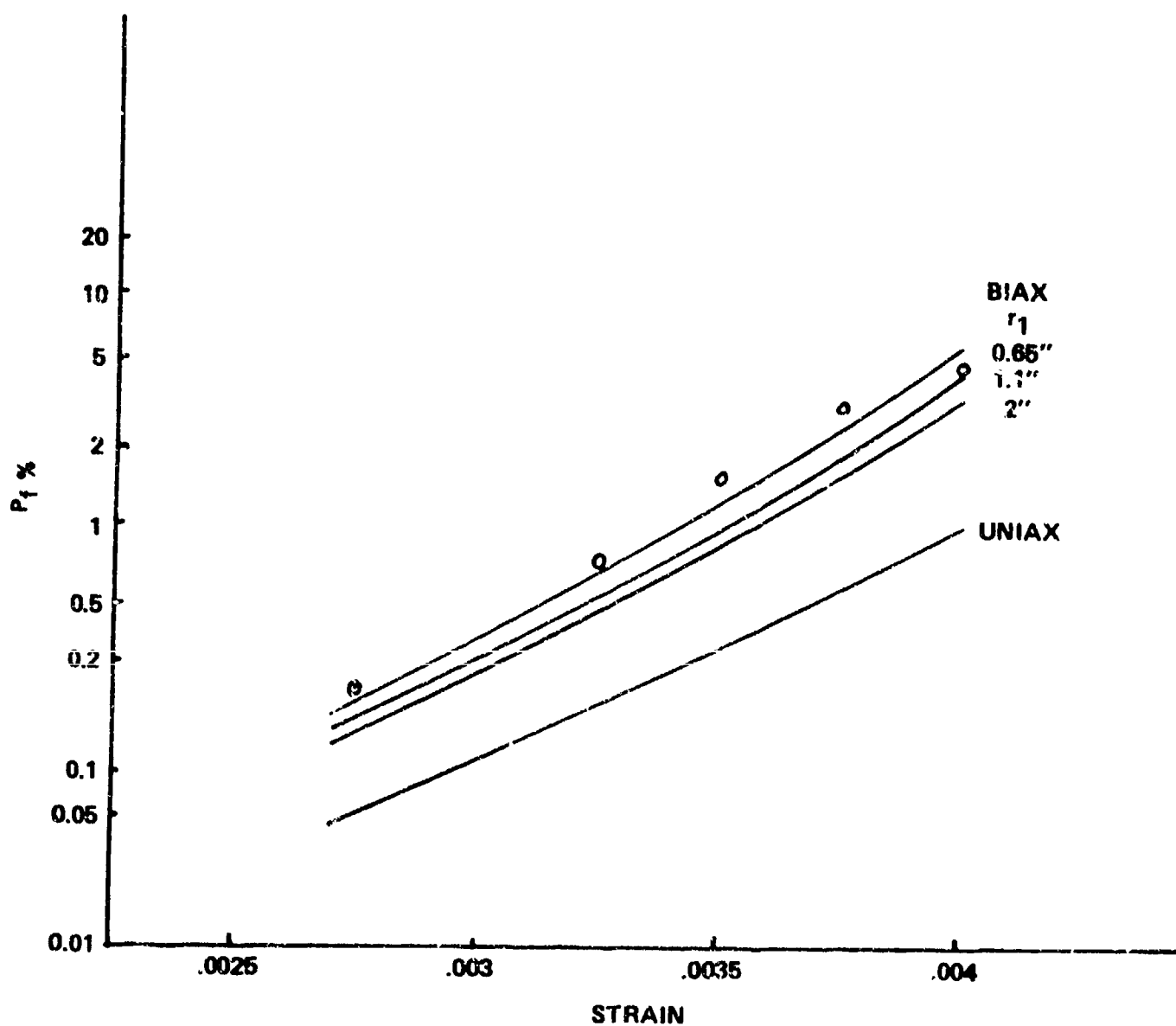
Figure 16. Theoretically Determined Probability of Fracture of 0.07 in^3. ATJS Graphite Specimens in Uniaxial and Various Biaxial Tensions. (Circles Found by Applying Eq. (20) to the Smoothed Data in Figure 17).
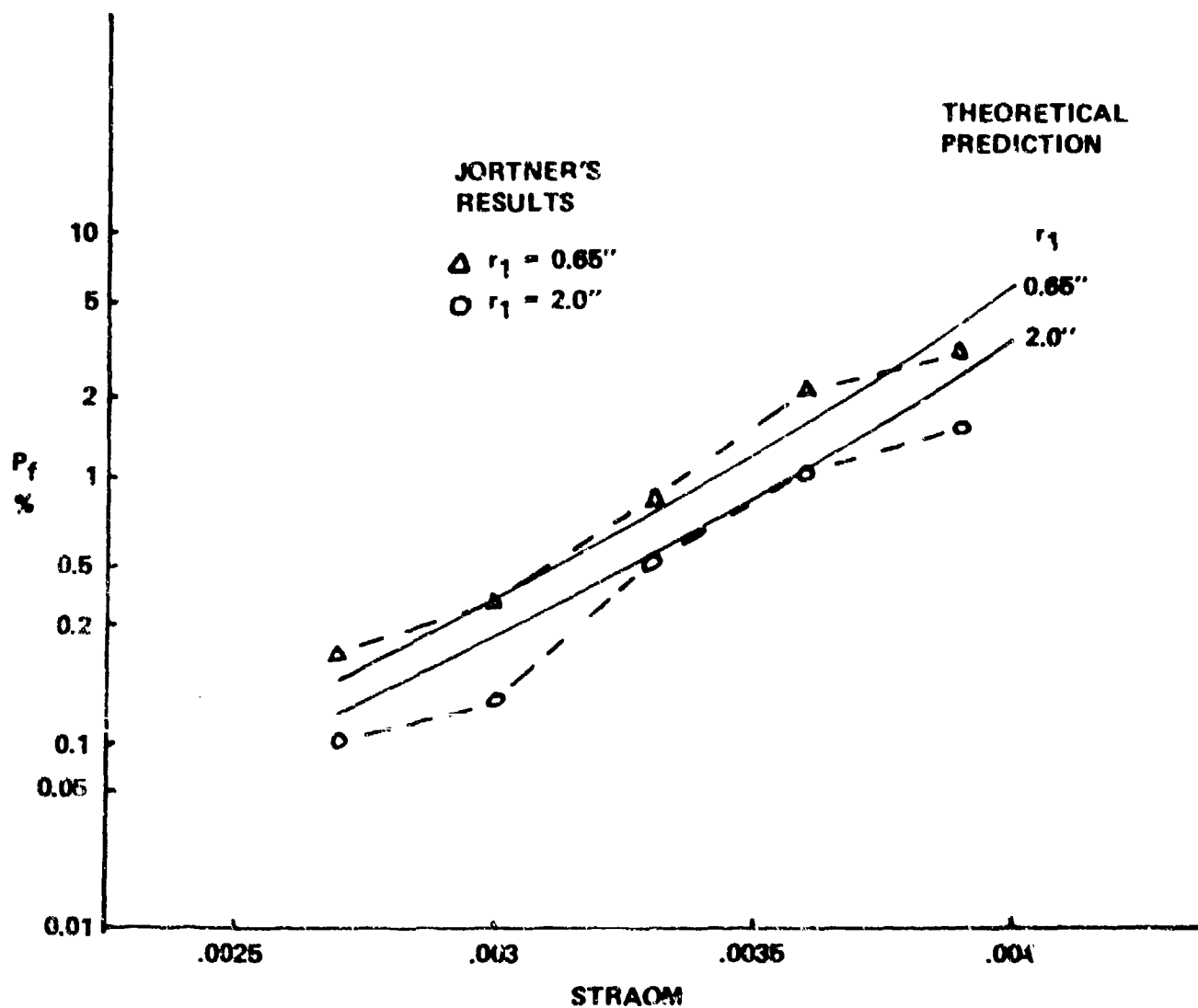
Figure 16. Probability of Failure of 0.07 in^3. Specimens of ATJS Graphite in Biaxial Loading Corresponding to that in Complete Disk and in Inner 0.65". Present Results Compared with Those of Jortner.

The first difference noted is that the curves just calculated are nearly straight lines on probability paper, whereas the curves of Fig. 3 are quite irregular The reason for this turns out to be that in effect, Reference 1 processes bar graph data with the aid of the equation

$$\Delta P_f(\epsilon) = \frac{\Delta N}{M(\epsilon)} P_s(\epsilon) \tag{20}$$

where ΔN is the number of failures in a chosen strain interval and M is the equivalent number of specimens of 0.07 cubic inches contained in the total volume of ATJS that was strained to at least the value ϵ. If the equation is applied to smoothed data (see Fig. 17) we obtain for $P_f(\epsilon)$ for the case $r_1 = 0.65"$ the circles shown in Fig. 15. These ults are smoother and also closer to our theoretical calculation.

It is difficult to carry out an analogous treatment for $r_1 = 2"$ because the large scatter in the test data makes the smoothing process very uncertain. Accordingly we resort to a different approach.

From Table 1 we can construct the experimental plot of $P_f(\epsilon_{max})$ shown in Fig. 18. We then assume that an average k exists for probability of fracture as a function of strain level which satisfies the equation

$$P_f(\epsilon) = 1 - \exp\left[-\int \bar{k}' \, \epsilon_\theta^{m'} \, dV\right] \tag{21}$$

It can be verified from Table 3 that for $\omega = 4200$ rad./sec., the strain ratio is closely approximately by

$$\frac{\epsilon_\theta}{\epsilon_{max}} = 1 - 0.105 \, r^2 \tag{22}$$

Inserting this relation in Eq. (21) we obtain

$$P_t(\epsilon_{max}) = 1 - \exp\left[-\bar{k}' \, 2\pi t \, \epsilon_{max}^{m'} \int_0^2 r \, dr(1-0.105 \, r^2)^m\right] \tag{23}$$
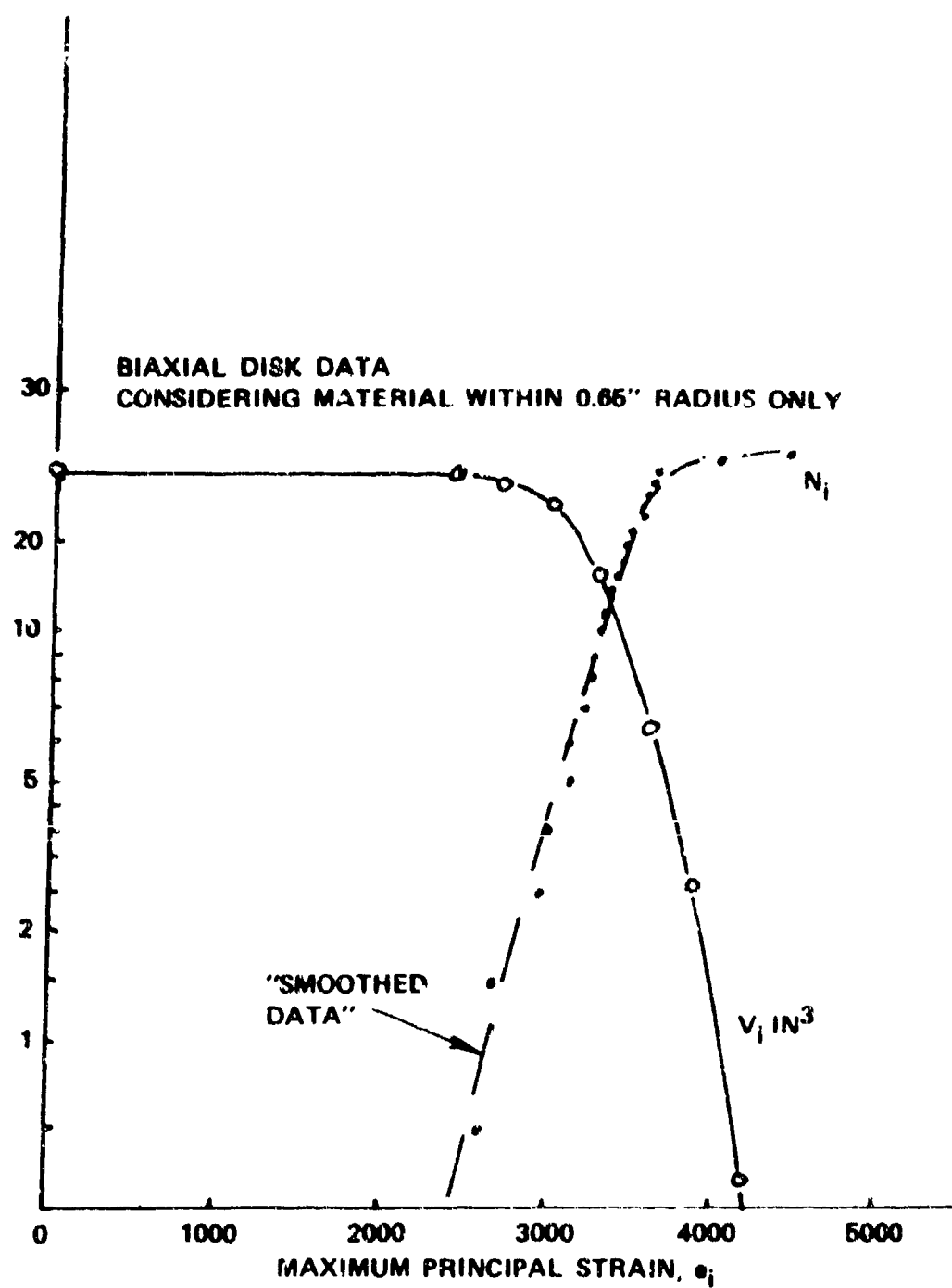
79

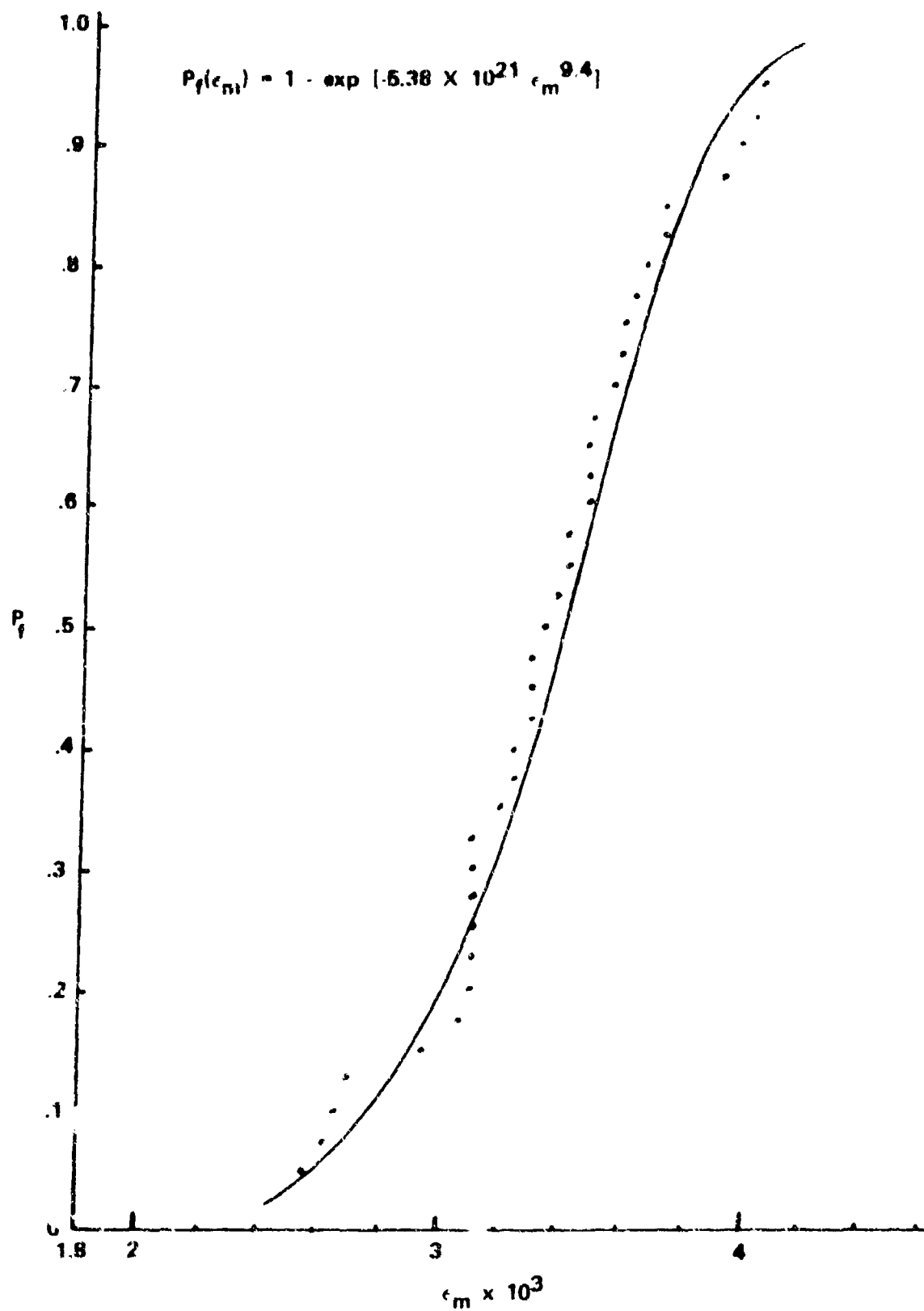Figure 17. Biaxial Disk Failure Data, Material Within x = 0.65 Inch.
(Adapted from Ref. 1)

$$P_f(\epsilon_m) = 1 - \exp\left[-5.38 \times 10^{21} \, \epsilon_m^{9.4}\right]$$

Figure 18. Probability of Fracture of Spinning ATJS Graphite Disks as a Function of Center Strain.

Carrying out the in$\underline{\quad}$ral and fitting the curve of Fig. 18 at the points corresponding to ω = 3800 rad./sec. and 4200 rad./sec. we obtain m' = 9.4 and $\bar{k}'$ = 7.7 × 10^{22}.

The theoretical curve corresponding to these values is shown in Fig. 18, and the fit is very satisfactory. Accordingly, we compute the probability of fracture as a function of strain for biaxially stressed 0.07 cubic inch specimens as deduced from data on the complete disks to be

$$P_f(\varepsilon) = 1 - \exp\left[- 0.07 \times 7.7 \times 10^{22} \varepsilon^{9.4}\right] \tag{24}$$

A similar treatment of the inner 0.65" of the disks leads to m' = 9.6, $\bar{k}'$ = 5.2 × 10^{23}. These results, shown as circles and triangles in Figure 19, turn out to be in excellent agreement with the theoretical prediction.

As a final check on the theory we calculate the frequency of fracture as function of distance from the center of the disk. The relative frequency is given by the integrand of the equation

$$P_f = 1 - \exp\left[- 2\pi t \ k_o \ \sigma_{max}^{12} \int_o^2 r \ dr(1-0.086 \ r^2)^{12} \frac{k}{k_o}\right] \tag{25}$$

Accordingly the suitably normalized function

$$F(r) = Kr(1-0.086 \ r^2)^{12} \ k\left(\frac{\sigma_r}{\sigma_\theta}, \ 12\right)/k_o \tag{26}$$

is plotted in Fig. 20. Also shown are the experimental data, as a plot of fracture location vs. rate of rotation, and the corresponding bar graph. The theoretical prediction is seen to be in excellent agreement with the bar graph.

DISCUSSION

As mentioned earlier, Reference 1 employed the principal strains at the locations of the fracture origins to reduce the disk failure data. No use was made of the statistical theory of fracture under biaxial loading. As a result,
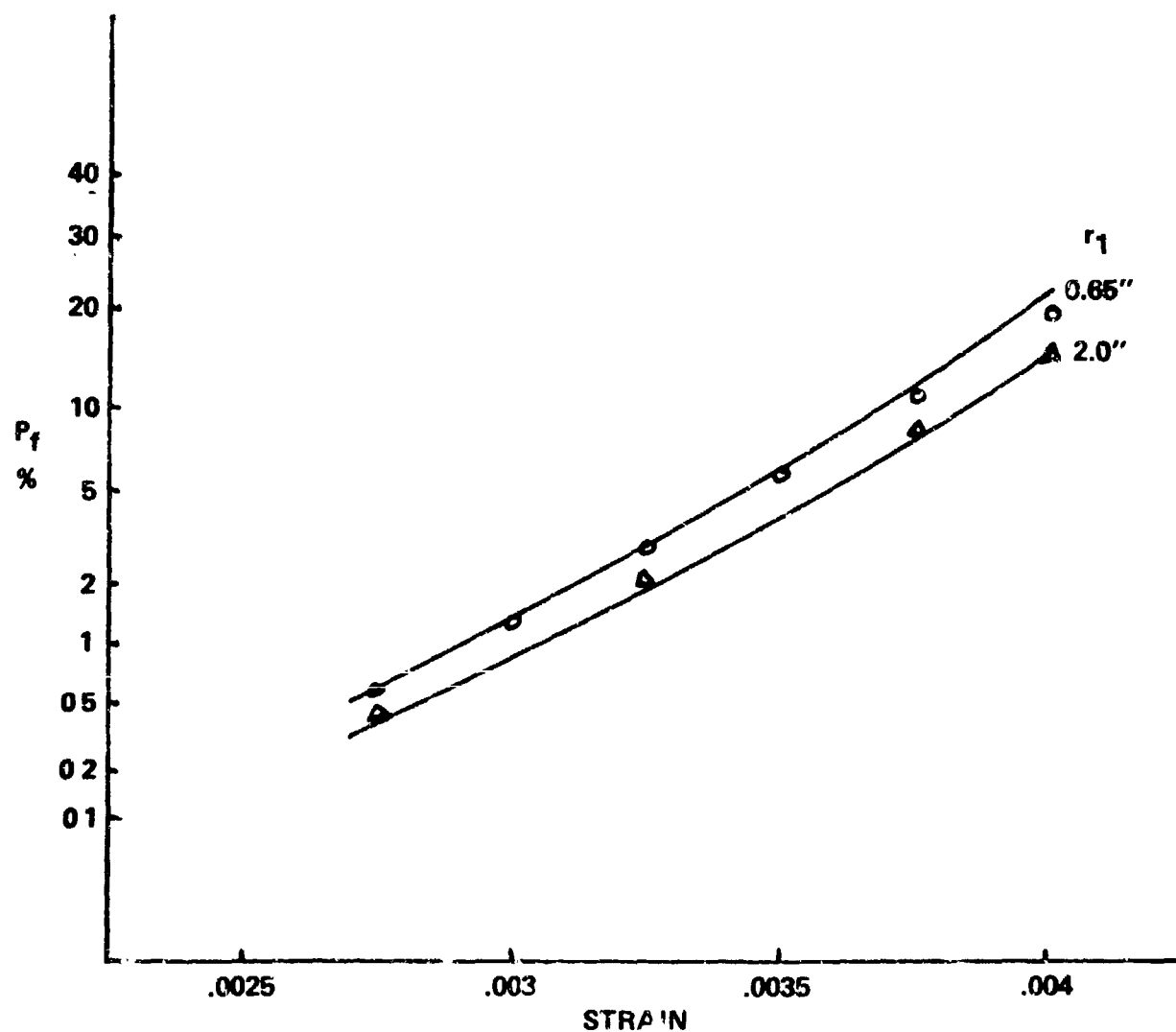
Figure 19. Probability of Failure versus Strain Curves Obtained from Stress Distribution in Table 2 and Theoretical Biaxial Fracture Statistics of Table 3. Circles and Triangles Obtained from Fracture Data of Table 1 and Strain Distribution of Table 2.
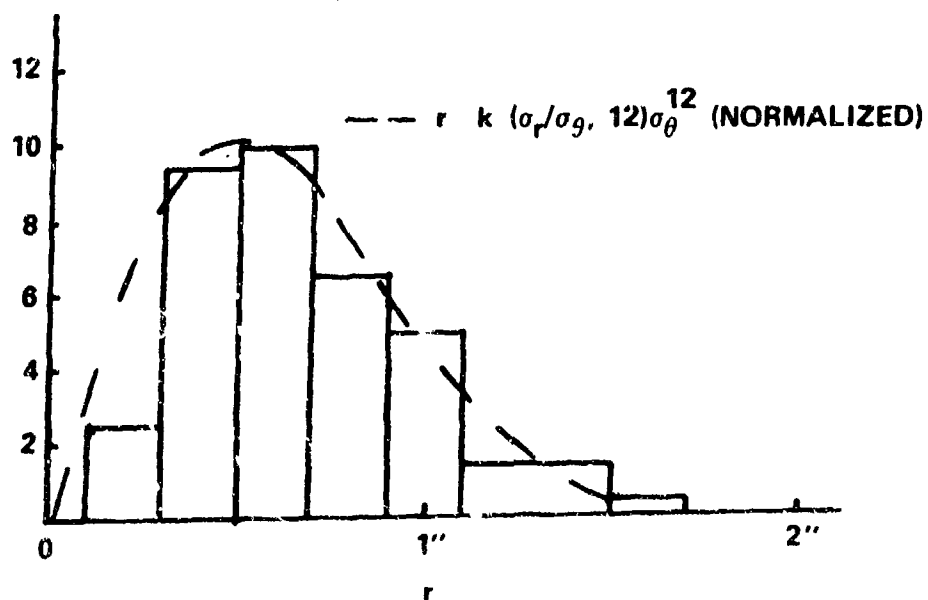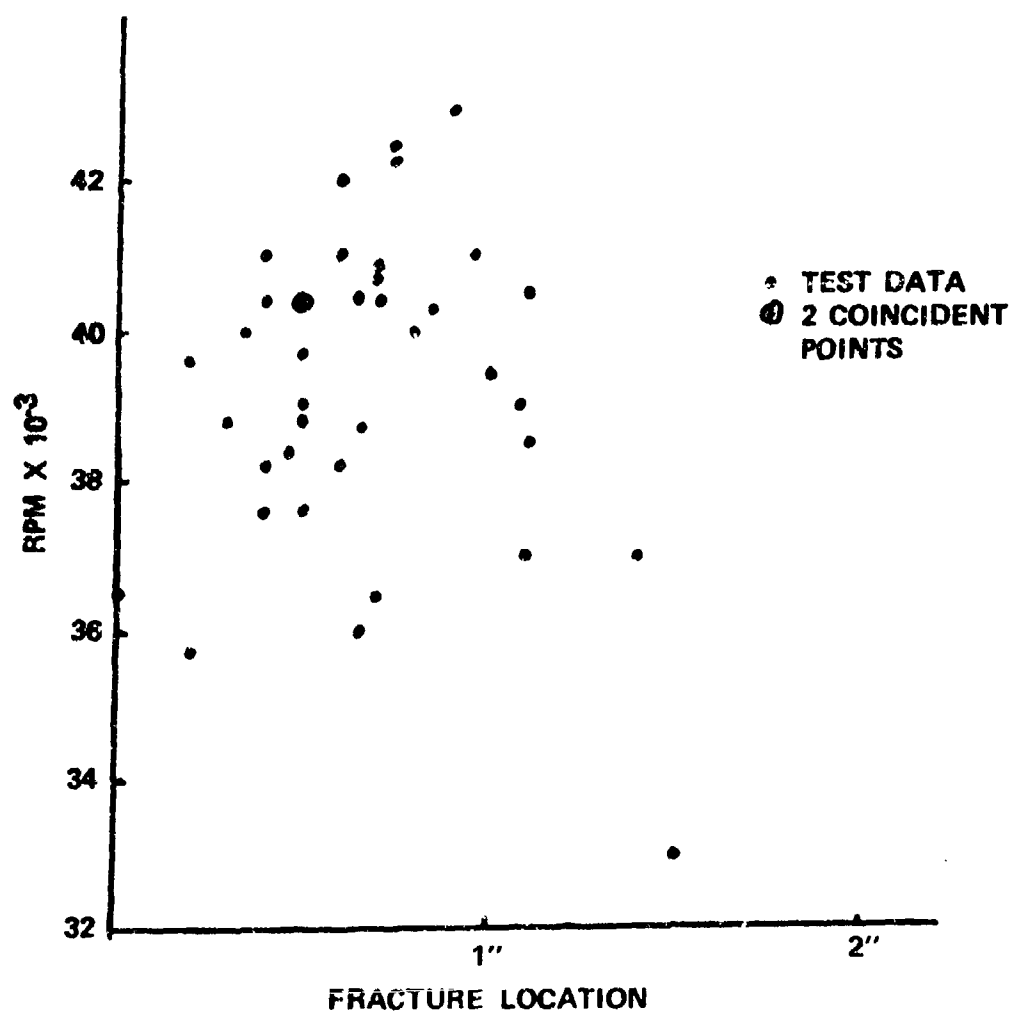
RPM X 10^{-3}

42

40

38

36

34

32

• TEST DATA
⊘ 2 COINCIDENT
    POINTS

1"   2"

FRACTURE LOCATION

12

10

8

6

4

2

0   1"   2"

r

— — r k $(\sigma_r/\sigma_\theta, 12)\sigma_\theta^{12}$ (NORMALIZED)

Figure 20. Fracture Frequency as a Function of Radial Location.

34

all that could be obtained was the probability of fracture vs. principal strain for several biaxial stress ratios that could only be approximately identified.

Application of the statistical theory of fracture together with the computed stress distribution has made it possible to deduce from the disk failure data the uniaxial failure statistics as well as the biaxial failure statistics for any stress ratio. This renders the results directly useful for structural applications. Agreement between theory and experiment was very good.

The computed stress distribution and the statistical theory of fracture under biaxial loading were also applied to determine the probability of fracture origin as a function of radial distance from the disk center, again obtaining very good agreement with experiment. Since the experiment did not provide a basis for checking polyaxial fracture statistics and stress distribution individually it cannot be asserted that these were unambiguously confirmed. But the fact that the theory of biaxial fracture statistics and the assumed polyaxial stress strain law combined to give so accurately the overall fracture statistics of complete disks or portions thereof as well as the radial distribution of the fracture origins and the strain at the disk center, is rather persuasive indirect evidence of the accuracy of both theoretical inputs.

The experimental data and the success of the theoretical analysis can also be regarded as evidence supporting weakest link theory as applied to graphite fracture. This is of particular interest in the light of findings in two earlier studies directed more specifically at looking into this question. In both studies attention was focussed on the volume effect. According to weakest link theory, the probability of fracture takes the form

35

$$P_f = 1 - \exp[-Vf(\sigma)]$$

where $f(\sigma)$ is a monotonic function, the form of which depends on the particular theory. Thus for a chosen value of P_f, the product $Vf(\sigma)$ is constant, and this relation determines the volume scaling. The earlier study[2] led to the conclusions that Weibull theory is qualitatively correct in predicting a lower mean fracture stress and smaller dispersion for larger specimens, but that the Weibull parameters are somewhat dependent on specimen volume. The second study[3] led to conclusions contradicting weakest link theory. It was reported in fact that "no size dependence of critical stress was found in the data obtained."

The present findings are compatible with those of the first study, but at variance with those in the second. A discussion of possible reasons for the negative findings in the second study is beyond the scope of the present paper. However it is apparent even without any analysis that the statement in quotes is not supported by the data in the ATJS fracture study of Reference 1. Here the maximum strains in the large disks at fracture ranged from 0.0023 to 0.0046 whereas in the small standard tensile specimens they ranged from 0.0038 to 0.0057.

The applicability of weakest link theory to the graphite disks is intuitively evident from the fact that in almost all cases it was possible to identify the flaw that initiated the fracture. In addition, the assumption of weakest link theory led to excellent detailed agreement with the experimental data. It may be that although not planned with that in mind, the test data of Reference 1, interpreted as in the present paper, constitutes one of the most definitive confirmations of weakest link theory available.

CONCLUSIONS

1.   Measured maximum strains in ATJS disks at various rates of rotation were in excellent agreement with calculations based on a polyaxial stress strain relation proposed by the present author.

2.   The corresp.nding stress analysis coupled to the theory of biaxial fracture statistics led to very good agreement with all the observed disk fracture data.

3.   The agreement between theory and experiment strongly supports the thesis that weakest link theory is applicable to the fracture of ATJS graphite.

4.   The success of the analysis illustrates how theory can be used for the purpose of enhancing the accuracy, consistency and practical usefulness of experimental results.

REFERENCES

1. Jortner, Julius "Biaxial Tensile Fracture of ATJ-S Graphite," Technical Report No. AFML-TR-74-262, March, 1975. Air Force Materials Laboratory, Wright-Patterson Airforce Base, Ohio.

2. Pears, C.D., and Starrett, H. Stuart, "An Experimental Study of the Weibull Volume Theory." Technical Report No. AFML-TR-66-228, March, 1968. Air Force Materials Laboratory, Wright-Patterson Air Force Base, Ohio.

3. Bausal, G.K., Duckworth, W.H., and Niesz, D.E., "Strength-Size Relationships in Ceramic Materials: Investigation of Pyroceram 9606," Technical Report No. 3, Office of Naval Research, November, 1974.

4. Batdorf, S.B., "A Polyaxial Stress-Strain Law for ATJS Graphite," SAMSO Report SAMSO-TR-75-39, January, 1975.

5. Batdorf, S.B., "Observations on Approximate and Exact Treatments of Fracture Statistics for Polyaxial Stress States," SAMSO Report SAMSO-TR-75-289, December, 1975.